University of Szeged

Faculty of Pharmacy

Institute of Pharmaceutical Technology and Regulatory Affairs

Head: Prof. Dr. Ildikó Csóka Ph.D.

DEVELOPMENT OF ANTIBIOTIC-LOADED *IN SITU* GELLING NANO DRUG DELIVERY SYSTEM FOR ENHANCED LOCAL NASAL THERAPY

Ph.D. Thesis

Sandra Aulia Mardikasari

Supervisor:

Prof. Dr. Ildikó Csóka Ph.D.

Dr. habil. Gábor Katona, Ph.D.

2025

PUBLICATIONS RELATED TO THE THESIS

I. **Mardikasari, S.A.**, Budai-Szűcs, M., Orosz, L., Burián, K., Csóka, I., Katona, G. (2022). Development of Thermoresponsive-Gel-Matrix-Embedded Amoxicillin Trihydrate-Loaded Bovine Serum Albumin Nanoparticles for Local Intranasal Therapy. *Gels*, 8, 750. **(Q2, IF: 4.6, Citation: 10)**

II. **Mardikasari, S.A.**, Katona, G., Budai-Szűcs, M., Sipos, B., Orosz, L., Burián, K., Rovó, L., Csóka, I. (2023). Quality by design-based optimization of *in situ* ionic-sensitive gels of amoxicillin-loaded bovine serum albumin nanoparticles for enhanced local nasal delivery. *International Journal of Pharmaceutics*, 645, 123435. **(Q1, IF: 5.3, Citation: 15)**

III. **Mardikasari, S.A.**, Katona, G., Sipos, B., Ambrus, R., Csóka, I., (2023). Preparation and Optimization of Bovine Serum Albumin Nanoparticles as a Promising Gelling System for Enhanced Nasal Drug Administration. *Gels*, 9, 896. **(Q1, IF: 5.0, Citation: 12)**

IV. **Mardikasari, S.A.**, Katona, G., Budai-Szűcs, M., Kiricsi, A., Rovó, L., Csóka, I. (2024). Mucoadhesive *in situ* nasal gel of amoxicillin trihydrate for improved local delivery: Ex-vivo mucosal permeation and retention studies. *European Journal of Pharmaceutical Science*, 202, 106897. **(Q1, IF: 4.3, Citation: 1)**

OTHER PUBLICATIONS

I. **Mardikasari, S.A.**, Sipos, B., Csóka, I., Katona, G. (2022). Nasal route for antibiotics delivery: Advances, challenges and future opportunities applying the quality by design concepts. *Journal of Drug Delivery Science and Technology*, 77, 103887. **(Q1, IF: 4.5, Citation: 13)**

II. Himawan, A., **Mardikasari, S.A.**, Katona, G., Vora, L.K., Pandya, A.K., Permana, A.D., Abu Ershaid, J.M., Larraneta, E., Patravale, V. (2024). Challenges and progress in nose-to-brain drug delivery. In: A. Kumar Singh., V. K. Chaturvedi, & J. Singh (Eds.), *Nanoarchitectonics for brain drug delivery* (1st ed., pp. 71−105). United States of America: CRC Press.

III. **Mardikasari, S.A**., Katona, G., Sipos, B., Csóka, I., (2024). Essential Considerations towards Development of Effective Nasal Antibiotic Formulation: Features, Strategies, and Future Directions. *Expert Opinion on Drug Delivery*, 21, 4. **(Q1, IF: 5.0, Citation: 1)**

IV. **Mardikasari, S.A**., Katona, G., Csóka, I., (2024). Serum albumin in nasal drug delivery systems: exploring the role and application. *Pharmaceutics*, 16, 1332. **(D1, IF: 4.9, Citation: 4)**

V. **Mardikasari, S.A**., Katona, G., Csóka, I., (2025). Bovine serum albumin nanoparticles: a promising platform for nasal drug delivery. *Expert Opinion on Drug Delivery*, 22, 1. **(Q1, IF: 5.0, Citation: 1)**

PRESENTATIONS RELATED TO THE SUBJECT OF THE THESIS

A) Oral presentations

I. **Mardikasari, S.A.,** Csóka, I., Katona, G., (2022). Development of *in situ* mucoadhesive-thermosensitive gel of amoxicillin for intranasal delivery, *IV. Symposium of Young Researchers on Pharmaceutical Technology, Biotechnology and Regulatory Science*, Szeged, Hungary.

II. **Mardikasari, S.A.**, Budai-Szűcs, M., Orosz, L., Burián, K., Csóka, I. Katona, G. (2023). Application of albumin-based nanoparticles integrated with thermoresponsive gel systems for enhanced nasal delivery of amoxicillin, *V. Symposium of Young Researchers on Pharmaceutical Technology, Biotechnology and Regulatory Science*, Szeged, Hungary.

III. **Mardikasari, S.A.**, Katona, G., Budai-Szűcs, M., Sipos, B., Orosz, L., Burián, K., Rovó, L., Csóka, I. (2024). Development of *in situ* ionic-sensitive nasal gels of amoxicillin-loaded albumin nanoparticle applying QbD-based optimization for improved local delivery, *VI. Symposium of Young Researchers on Pharmaceutical Technology, Biotechnology and Regulatory Science*, Szeged, Hungary.

IV. **Mardikasari, S.A.**, Katona, G., Nodilo, L.N., Hafner, A., Kalogjera, L., Zadravec, D., Orosz, L., Burian, K., Balogh, G.T., Csóka, I. (2025). Development of *in situ* nasal gels of ceftriaxone-loaded albumin-based nanoparticles for improved treatment of bacterial meningitis, *VII. Symposium of Young Researchers on Pharmaceutical Technology, Biotechnology and Regulatory Science*, Szeged, Hungary.

B) Poster presentations

I. **Mardikasari, S.A.**, Budai-Szűcs, M., Orosz, L., Burián, K., Csóka, I. Katona, G. (2023). Albumin-based nanoparticles incorporated into thermosensitive gelling systems for improved local intranasal delivery of amoxicillin, *European Federation for Pharmaceutical Science Annual Meeting (EUFEPS),* Lisbon, Portugal.

II. **Mardikasari, S.A.**, Katona, G., Budai-Szűcs, M., Kiricsi, A., Rovó, L., Csóka, I. (2024). Intranasal Delivery of *in-situ* Mucoadhesive Gel of Amoxicillin: *Ex-vivo* Mucosal Permeation and Retention Studies. *The 5th EUGLOH Annual Student Research Conference,* University of Alcala, Alcala, Spain.

ABBREVIATIONS

ABR	Acute Bacterial Rhinosinusitis
ACE	Angiotensin Converting Enzyme
AMT	Amoxicillin Trihydrate
ANOVA	Analysis of Variance
API	Active Pharmaceutical Ingredient
BBB	Blood-Brain Barrier
BSA	Bovine Serum Albumin
$CaCl_2$	Calcium Chloride
CIC	Critical Ionic Concentration
CNS	Central Nervous System
C_{max}	Maximum plasma concentration
DLS	Dynamic Light Scattering
EDTA	Ethylenediaminetetraacetic Acid
EE	Encapsulation Efficiency
EHEC	Ethyl Hydroxy-Ethyl Cellulose
EMA	European Medicines Agency
EUCAST	The European Committee on Antimicrobial Susceptibility Testing
GG	Gellan Gum
G′	Storage Modulus
G″	Loss Modulus
HPLC	High Performance Liquid Chromatography

ICH	The International Council for Harmonization of Technical Requirements for Pharmaceuticals for Human Use
IN	Intranasal
J	Flux
Kp	Permeability coefficient
KCL	Potassium Chloride
LOD	Limit of Detection
MCC	Mucociliary Clearance
MW	Molecular Weight
NaCl	Natrium Chloride
NALT	Nasopharynx-Associated Lymphoid Tissue
NaOH	Sodium Hydroxide
NC	Negative Control
ND	Neurodegenerative Disease
Papp	Apparent Permeability
PC	Positive Control
PBS	Phosphate-Buffered Saline
PdI	Polydispersity Index
QbD	Quality by Design
SD	Standard Deviation
SNES	Simulated Nasal Electrolyte Solution
ZP (ζ)	Zeta Potential

TABLE OF CONTENTS

1. INTRODUCTION

Acute bacterial rhinosinusitis (ABR) is a widely spread disease with an incidence of 5–40 episodes per 1000 patients per year, generally affecting the adult population, yet it is not uncommon amongst infants and children below 18 years. The general therapeutical protocol includes large doses of amoxicillin (up to 1000 mg daily) with or without clavulanic acid and local treatment of sinusitis via nasal decongestants, saline solution, and if needed, steroidal nasal sprays [1,2] and prolonged therapy is required for up to 7 or 14 days [3,4]. However, oral administration of antibiotics can affect systemic circulation and potentially cause adverse reactions [5]. Also, the absorption rate of orally administered amoxicillin in a high dose, especially twice-daily dosing, showed non-linearity in C_{max} and has the potential to result in low antimicrobial efficacy due to insufficient bioavailability [6,7]. Therefore, topical delivery of amoxicillin to the nasal mucosa can be a viable choice to provide better outcomes.

Moreover, another considerable factor that can potentially influence the treatment effectiveness is the lack of patient adherence, resulting in drug resistance and insufficient therapy. Thus, in this circumstance, there is a high demand for an effective antibiotic therapy, for which technological solutions can be proposed such as choosing the most effective administration route, i.e., achieving targeted therapy and formulating value-added dosage forms by means of nano-technology and protein-based drug delivery systems.

Furthermore, intranasal drug administration has emerged as an alternative and promising route in delivering a drug, which provides many advantages, such as the non-invasive way of drug administration, avoiding first-pass metabolism, which in turn can achieve higher bioavailability, lower dosing of administration, and accessibility for local and systemic therapeutic purpose as well as for brain targeting [8]. However, nasal route delivery poses many challenges, and the most significant is nasal mucociliary clearance [9]. Therefore, a proper design of nasal drug formulation is particularly required to overcome the challenges following nasal route application and deliver the drug effectively.

In this case, a suitable nanocarrier system is of great importance to apply. The *in situ* stimuli-sensitive delivery systems appear promising for the delivery of antibiotics to the nasal passage. This system can be employed to prevent rapid clearance of the formulation from the nasal cavity and enhance its residence time while releasing the active substance locally. Therefore, the utilization of *in situ* gelling system to administer antibiotic into the nasal cavity could be a promising approach to achieve better local therapeutic effect as well as establish the proper use of antibiotic.

2. AIMS

This Ph.D. work aimed to prepare novel and innovative formulations of amoxicillin-loaded bovine serum albumin (BSA) nanoparticles incorporated into *in situ* gelling polymer matrix for enhanced local nasal therapy of antibiotic for ABR treatments. In order to circumvent nasal challenges and achieve desired properties of formulation for local therapy in the nasal cavity, the combination of nanocarrier system and *in situ* gelling polymer can be utilized as it has shown many great potentials for drug delivery. Thus, the research work was carried out with the aims of these following steps:

I. To optimize the composition of albumin-based nanocarrier system via factorial design, in order to obtain adequate solubility and stability to load the antibiotic drug, generating suitable properties for nasal administration, such as nanosized formulations with good zeta potential and polydispersity index (PdI), as well as the pH and osmolality.

II. To develop amoxicillin-loaded albumin nanoparticles with high drug entrapment efficiency and incorporate them into thermo-responsive and ionic-sensitive *in situ* gelling matrices, then perform appropriate investigation to compare their characteristics according to intranasal administration.

III. To evaluate the *in vitro* drug release behavior of the *in situ* stimuli-sensitive nasal gel AMT formulations in simulated nasal electrolyte solution as the release medium, in order to mimic the condition in the nasal cavity.

IV. To investigate the *in vitro* antibacterial activity to confirm that the antibiotic substance (amoxicillin) in the *in situ* stimuli-sensitive nasal gel formulations can maintain its inhibitory activity against five common ABR pathogens, ensuring the efficacy of the *in situ* nasal gel formulation of amoxicillin.

V. Finally, we aimed to determine the mucosal permeation and retention properties through the *ex vivo* mucosal permeation and retention studies employing human nasal mucosa tissue in order to ensure the application of the developed *in situ* nasal gel formulation of amoxicillin is appropriate for local therapeutic purposes.

3. THEORETICAL BACKGROUND

3.1. Acute Bacterial Rhinosinusitis

Acute rhinosinusitis, also referred to as acute sinusitis, is a four-week-long inflammation of the nasal cavity and paranasal sinuses [10]. Acute sinusitis is further classified according to presumed cause as either acute bacterial rhinosinusitis (ABR) or acute viral rhinosinusitis. The time course and duration of compatible symptoms are typically used to distinguish ABR from viral infection. ABR is defined by either an onset of severe symptoms, like the presence of purulent nasal discharge with nasal obstruction such as facial pain, fullness, and pressure, including a high fever for three days, or a worsening of symptoms (or double worsening) or persistence of symptoms for at least ten days. ABR is one of the most common infections treated by primary care providers. Beyond the nasal cavity and paranasal sinuses, bacterial sinusitis can spread directly to the orbit or surrounding tissues, or it can hematogenously or directly affect the central nervous system (CNS). Complications are uncommon but can be potentially serious, indeed life-threatening. ABR may also lead to the CNS infections, such as meningitis, subdural empyema, epidural abscess, or brain abscess [11]. Patients with any of the signs or indications proposing a complication of ABR ought to be urgently referred to an emergency department for assessment and management.

3.1.1. Pathogens of Acute Bacterial Rhinosinusitis

Normal bacterial flora, which includes potential pathogens that can cause respiratory tract infections, including sinusitis, colonizes the upper respiratory tract, including the nasopharynx. During viral respiratory infections, these possible pathogens can cause sinus infections by moving from the nasopharynx into the sinus cavity [12]. ABR complicates 0.5–2.0% of cases of the common cold and is most frequently a consequence of viral infection. However, other conditions like allergies, immunological dysfunction, ciliary dysfunction, sinus anatomic narrowing, or poor dental health can also make people more susceptible to ABR.

Furthermore, *Moraxella catarrhalis*, *Haemophilus influenzae*, *Staphylococcus aureus*, *Streptococcus pneumoniae*, and *Streptococcus pyogenes* are the most frequently found bacteria linked to ABR [13]. Anaerobic bacteria and microaerophilic streptococci are frequently detected if the ABR comes from an odontogenic source. A single pathogen is typically found in high concentration when a sinus culture is positive in a patient with ABR, though two pathogens may be found in high concentration in about 25% of the patients. Anaerobic bacteria derived from the oral flora may become the predominant pathogens if the acute infection does not resolve. Through serial culture during the course of the infection, these phases were shown in patients with maxillary sinusitis.

Nonetheless, cultures continue to be useful in certain clinical settings, such as nosocomial or complex ABR. In this case, ABR is characterized by purulent nasal drainage rhinosinusitis (anterior, posterior, or both) that lasts for less than four weeks, along with facial pain, pressure, fullness, or nasal obstruction (such as congestion, blockage, or stuffiness).

3.1.2. First line treatment

The utilization of antibiotics for the treatment of ABR can help shorten the course of ABRS, however it must be taken into account that potential benefit is greater than the adverse effects. Oral amoxicillin (1000 mg three times daily) or amoxicillin-clavulanate (875/125 mg twice daily or 500/125 three times daily) for 5-10 days has been recommended as the first-line treatment for ABR in adults [2], with consideration based on the resistance patterns in the community. Amoxicillin-clavulanate is preferred in communities where *Haemophilus influenzae* and *Moraxella catarrhalis* isolates have a higher prevalence of beta-lactam resistance, while macrolides and trimethoprim-sulfamethoxazole are not suggested because of a significant prevalence of *S. pneumoniae* resistance, as well as for trimethoprim-sulfamethoxazole and also *H. influenzae* resistance [11]. In this case, all dosages are for patients with adequate kidney function.

High doses of amoxicillin with clavulanate (2 g/125 mg twice daily) is recommended for adults with specific risk factors for antibiotic resistance [3], such as living in areas where the prevalence of penicillin-non-susceptible S. pneumoniae is higher than 10%, being older than 65, being hospitalized within the last five days, using antibiotics within the past month, having multiple comorbidities and immunocompromise, or other severe infections [3]. However, amoxicillin-clavulanate is the most commonly prescribed antibiotic that results in hospitalization for drug-induced liver disease and is known to cause adverse antibiotic events related to the gastrointestinal tract. Meanwhile, amoxicillin showed comparable effectiveness to amoxicillin-clavulanate for treating acute sinusitis, with fewer side effects related to the gastrointestinal tract. Therefore, amoxicillin is a viable choice for adults with acute sinusitis that require antibiotics therapy [1].

3.2. Nasal drug delivery systems

Intranasal delivery is a non-invasive route of administration that possesses many advantages, including ease of application, rapid onset of action, avoidance of the first-pass effect, availability for local and systemic delivery of drug and applicable for various kinds of formulation [8]. Nevertheless, this route is also challenging with several factors that must be well-considered. As for the nasal conditions themselves, the limitations in nasal cavity like the highly effective mucociliary clearance, small administrable volume, nasal pH, and facilitated membrane permeability, may become problems when preparing nasally applied drugs. Therefore, to overcome

this obstacle, numerous strategic approaches became choices, one of which is the formulation of the residence time prolonging *in situ* mucoadhesive gel formulations to avoid rapid drug clearance from the nasal passages. Furthermore, other factors that could possibly influence the formulation of intranasal drug delivery can be derived from the drug substance or active ingredient. In the case of antibiotics, their stability is the primarily important issue that must be carefully considered before the formulation is established since many antibiotics are physicochemically unstable in aqueous solutions or when exposed to the air or the light. For this purpose, a number of solid-form antibiotic preparations have been developed, which will be dissolved at the time of use [14].

Principally, nose is a unique organ for the smell function, which consists of two nasal cavities separated by the inner wall, known as nasal septum. In humans, the size of the nasal cavity is 12–14 cm long and 5 cm high, with the total volume approaching 15-16 cm^3 [15]. The total intranasal volume significantly conforms with the size of nostril openings [16] and the nasal airflow is slightly dominant inside the left nostril compared to the right one [17]. Interestingly, the shape and size of nasal are different across populations [18]. Nasal cavity has several major parts, including nostrils, vestibule, atrium, respiratory region (the turbinates), olfactory region, and nasopharynx as shown in Figure 1.

The nasal channel passes via the nostrils and runs about 12 cm from the vestibule to the nasopharynx area [15]. The nasal vestibule, as the anterior part, is the smallest cross-sectional area extending from the nostrils' opening and connecting the nose to the outer environment. The mean area of total nostril opening is around 0.3 – 0.4 cm^2 , which is found to be more prominent in men than women [16]. The surface of nasal vestibule is covered with skin containing vibrissae or hair to filter the large particles. These region cells are dominated by keratinized, squamous, and stratified epithelial cells with sebaceous glands [19,20]. Dehydration causes no problem for the nasal vestibule because of its physiological properties, and it can withstand shocks from harmful compounds of the environment. Permeation of substance through nasal vestibule is extremely limited. Hence, the nasal vestibule is not a preferred region for drug administration as well as drug absorption [19].

Drug absorption is optimal in the respiratory mucosa region. The respiratory region is divided into three projections originating from the septum, called turbinate or conchae. These turbinates are located at the lateral wall of the nose, namely the superior, middle and inferior turbinate. The space between each turbinate is called the meatus. An essential anatomical region for the function of anterior paranasal sinuses is the middle meatus. Acute and chronic sinusitis can be caused by anatomic anomalies or inflammatory mucosal in this location [21].

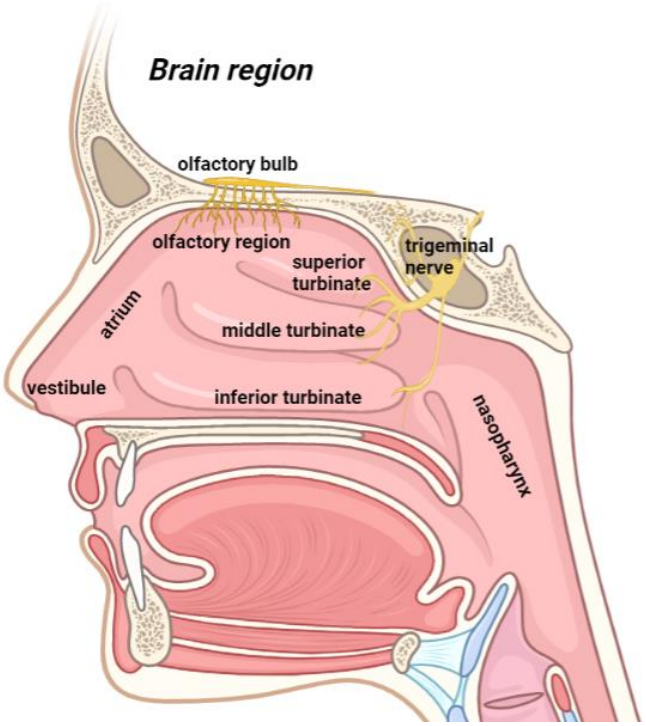

Figure 1. Illustration of human nasal cavity on a sagittal view [14].

3.2.1. Therapeutic purposes of nasal drug delivery

Nasal route has emerged as a valuable way for drug delivery with the purpose of local action, systemic transport, and nose-to-brain therapeutic effect due to simple access, high vascularized and has protective epithelium [9]. Intranasal delivery mechanism as explained in Figure 2 is capable of providing absorption pathway to the paranasal sinuses, brain and systemic. Nasal cavity is mainly used for therapy of local diseases in the upper airway tract, such as nasal infections, nasal congestion, nasal allergic rhinitis, nasal sinusitis and several lung infections (nose-to-lung delivery) [22,23]. The best-targeted area for this local treatment is the middle meatus since this area is connected with the opening of sinuses. Smaller doses than systemic administration can be applied for direct drug administration at the site of action.

The main characteristic of locally acting drugs requires a prolonged residence time. In addition, for vaccination delivery through nasal, the nasopharynx-associated lymphoid tissue (NALT) area is beneficial as a target site because it expresses higher immunogenic responses than other nasal regions. Further, a recent study described that for SARS-CoV-2 vaccination, the administration should be targeted to the posterior two-thirds of the nose as the receptor (Angiotensin - Converting Enzyme 2 or ACE2) are extremely populated in this nasal epithelial cell (ACE2 - rich region) [24].

Although the respiratory area is the primary site for absorption of nasal sprays, the drug retention period is limited due to the mucociliary clearance. After about 30 minutes, the majority of

the drug formulation in the posterior part of the respiratory region dropped into the nasopharynx. Nasal delivery in the anterior portion of this region, on the other hand, can achieve a longer residence time, which is preferable for systemic drug absorption.

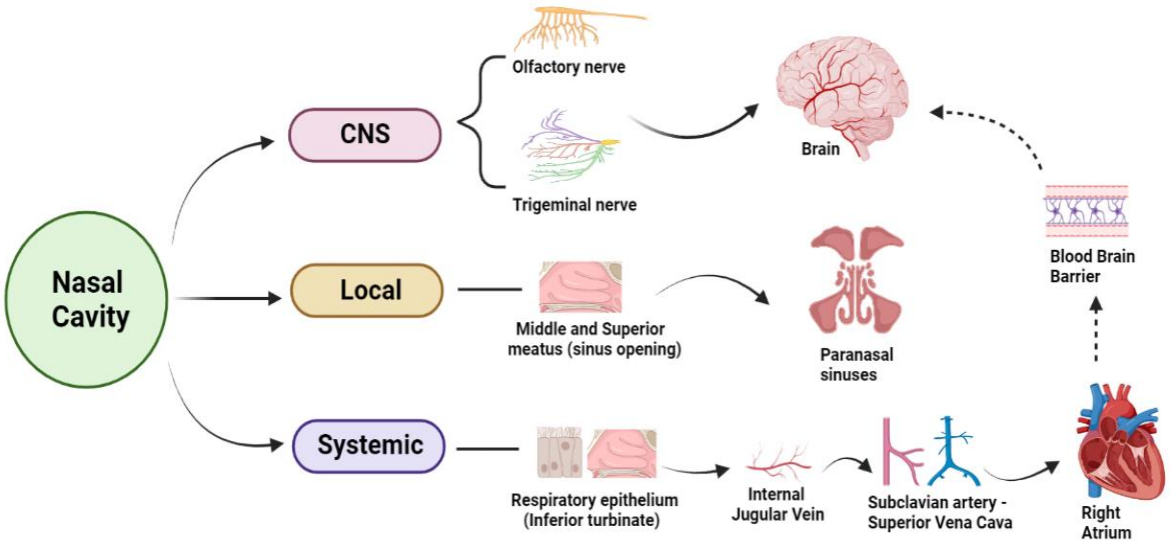

Figure 2. Schematic diagram of nasal drug delivery pathway [14]

3.2.2. Challenges and formulation strategies

Nasal drug delivery potentially provides greater comfort and safety by delivering drugs directly to the site of action. Compared to other administration methods, it is a non-invasive and painless way of delivery that encourages better compliance. However, this route has several limitations that able to lower the efficiency of intranasal route. There are numerous physiological and physicochemical barriers that can significantly influence nasal drug delivery [14] .

Nasal mucociliary clearance is an important function in keeping the health and defense mechanism in the nose. The mucociliary clearance is a protection system of the lower airway tract from dust and other particles. About 80% of particles with the size larger than 12.5 µm will be captured by the mucus that cover nasal epithelium and filtered out of the air before entering the pharynx [25,26]. The clearance mechanism involves the cilia and mucus which are produced by goblet cell. Nasal mucus acts as a continuous layer covering the nasal cavity to moisten and protect the nasal epithelium. The mucus blanket can be transferred from the anterior part of the nose to the nasopharynx. The mucociliary clearance is renewed every 15 − 20 min, constantly, at the rate up to 20 mm/min with the moves to the posterior region of the nose. Ciliary beating transports the inhaled particles, bacteria and viruses which previously trapped in the mucus and then move backward to the pharynx, where it can be swallowed or expelled. Different from the posterior part, the anterior part of the inferior turbinate the clearance system is by moving forward to the proximal part of the

nose for the removal mechanism. Nasal mucociliary clearance process can reduce drug residence time in the nasal cavity and decrease the drug permeation through the nasal mucosa [9,27].

Also, as the nasal cavity has a minimal volume in size, only a small amount of drug can be instilled, and the drug must be administered at a specific site of the turbinates and olfactory region to precisely achieve the intended effect of therapy. The geometry of nasal cavity, site of drug deposition and patient's head position during administration extremely affects drug absorption through the neuronal system and raises significant challenges for nasal drug delivery. Moreover, Particle size is essential in intranasal delivery. Also, the particle size should be less than 200 nm to facilitate absorption through the epithelium. Drug deposition in the nasal cavity is highly depends on the physical characteristics of the drug particles, ventilation, and anatomy of the respiratory system.

Finally, due to these challenges, several approaches have been employed to overcome nasal drug absorption issues. These actions range from the development of formulation strategies to devices used for nasal application, in which the primary purposes are to avoid the limit and to improve drug absorption through the nasal route administration [14].

3.3. In situ gelling system

In situ gelling system are liquid formulations which create a solid-like depot when applied topically or injected into the body. Over the past 20 years, they have drawn more and more attention as a desirable class of responsive drug delivery systems for a range of pharmaceutical and biomedical applications. Because they are easier to prepare and have lower production costs, they are preferred over conventional injectable depot systems like wafers or implants. This is because they can be self-administered using autoregulators, facilitate controlled release of incorporated therapeutic agents, which lowers the frequency of dosing and prevents therapeutic failure or undesirable side effects, and are injectable using smaller gauge needles. These system's low viscosity state under ambient conditions makes topical administration appealing as well [28].

In situ gelling systems are a carrier system that can undergo a sol-to-gel transition triggered by external stimuli of the nasal physiological environment, such as temperature, pH, and ionic condition. Among the many benefits of *in situ* gelling systems are their high drug-loading efficiency, sustained release profile, increased nasal absorption, extended retention period, decreased frequency of doses, and enhanced patient compliance. Based on the polymers used in the formulation, the gelation mechanism of the *in situ* gels greatly affects its performance. The selection of the type of polymer intended to be used in the formulation is crucial because it relates to the expected stimulus-response [28,29].

3.3.1. In situ gelling polymers

According to the stimuli-sensitive behavior there are generally three types of *in situ* gelling polymers: thermo-sensitive, ionic-sensitive, and pH-sensitive polymer. The thermo-sensitive polymer facilitates the transformation of the sol-to-gel upon temperature change ($25 - 37\ ^{\circ}C$) following instillation into the nostrils. The polymers that are commonly used in this group are Poloxamers® (P407 and P188), chitosan, ethyl (hydroxyethyl) cellulose (EHEC), and xyloglucan [29–31]. Meanwhile, the pH-sensitive polymers have the ability to convert the solution into the gel as the pH changes. The main polymer used as a pH-sensitive agent is Carbopol® which can maintain the pH in the range of $4 - 5.5$. Moreover, the last type of polymer, the ionic-sensitive polymer can performs sol-gel transition in the presence of environmental ionic influence. Gellan gum and pectin are ionic-sensitive gelling agents which perform interaction with the cations in the nasal fluid leading to the formation of gel structure [29].

3.3.2. In situ thermo-responsive polymer

One of the most attractive thermo-responsive polymers that have been widely exploited in the development of *in situ* gelling systems is Poloxamer 407 (P407). P407 is composed of a triblock copolymer of hydrophilic polyethylene oxide (PEO) and hydrophobic polypropylene oxide (PPO) in a structure: PEO-PPO-PEO. Due to its amphiphilic nature, P407 performs a reversible thermal characteristic. At a low temperature, the P407 molecular structure is surrounded by the hydrated layer and it can easily undergo spontaneous micellization due to the self-assembly mechanism. As the temperature rises, the hydrogen connection between water and the hydrophilic chain of PEO dissipates, resulting in the rearrangement of a micellar structure and the formation of bigger, hexagonal-shaped micelles [32]. The nasal application of P407 can promote a prolonged residence time of the entrapped drug in the nasal cavity and improve its bioavailability. The combination of thermosensitive polymers and nanocarrier systems can be considered, as it has shown great potential for controlled release properties in nasal application [28,33].

3.3.3. In situ ionic-sensitive polymer

Gellan gum, a linear, anionic exopolysaccharide made by Sphingomonas elodea, is one of the well-studied ionic-sensitive polymers. It is made up of the repeating units α-L-rhamnose, β-D-glucose, and β-D-glucuronate in molar ratios of 1:2:1. It proved to be a useful excipient when designing drug delivery vehicles for oral, ophthalmic and nasal delivery [29]. The polymer begins to gel when it is exposed to physiological concentrations of cations, which are found in physiological fluids like nasal fluid.

Gellan gum interacts with the simulated nasal fluid after being instilled into the nasal cavity,

creating a crosslinked network that further promotes gel formation. Thus, the ionic composition of nasal fluid ionic composition, pH, and volume can significantly affect gellan gum delivery properties [34]. The nasal fluid in a healthy nose has a volume of approximately 100 μL and a pH of 6.4, which can rise to 7.4 in the event of an infectious disease. Gellan gum has mucoadhesive properties, but because these are dependent on weak forces like hydrogen bonds and van der Waals forces, they are still insufficient to extend mucosal residence time. Therefore, the combination with other mucoadhesive polymer, such as albumin-based nanoparticles might then improve the mucoadhesiveness to further intensify the contact to the mucosa and consequently prolong the residence time.

3.4. Antibiotic delivery through nasal route administration

The nasal route has been used to deliver a wide range of small compounds and biological macromolecules such as peptides, proteins and vaccines. Also, common diseases treated using nasal dosage forms include allergic and infectious rhinitis, sinusitis, nasal epithelial lesions, and rhino-sinusitis. Therefore, antibiotic substances has the potential to be delivered directly to the nasal cavity for the treatment of acute bacterial rhinosinusitis. In this case, the utilization of the nasal route for delivering antibiotic substances can substantially reduce the risk of antibiotic resistance due to the inappropriate use of antibiotics.

In this circumstances, one of the most crucial global health challenges related to antibiotics is the resistance threat. Antibiotic resistance represents the condition when the pathogens establish an ability to resist the action of a certain antibiotic. Consequently, the antibiotics become ineffective for the treatment and lead to higher treatment costs, longer hospital stay, more complications, and even an increase in the number of deaths. The antibiotic resistance threat has emerged as the biggest public health problem worldwide [35]. Moreover, many efforts and concerns are established as prevention strategies for combating antibiotic resistance. One of the prioritized areas that plays an essential role is the improvement of proper antibiotic use.

Therefore, nasal delivery appears to be a reliable alternative route to oral administration of antibiotic. Nasal passage has a large surface area for absorption and is highly vascularized, allowing faster drug absorption without undergoing gastrointestinal and hepatic metabolism, which results in a higher drug bioavailability [9]. Besides that, therapeutic doses could be potentially lower to achieve optimal therapeutic efficacy. The frequency of use might also be reduced, as nasal delivery is able to provide high bioavailability on the target site, i.e. for local therapy in the nasal cavity. In line with this, antibiotic delivery through the nasal route can potentially minimizes the systemic adverse reactions that commonly arise when antibiotics are given orally, for example, nausea, diarrhea, rash, dizziness, etc, since the nasal delivery pathway completely bypasses the

gastrointestinal and hepatic first-pass metabolism, thus prevents the drug for being metabolized by cytochrome P450 enzymes, avoiding systemic adverse effects to occur.

Overall, nasal route administration provide great advantages for delivering antibiotics substances, as summarized in Table 1. Therefore, with respect to the effective delivery of an antibiotic substance through the nasal route, a proper understanding is hugely required in manufacturing intranasal antibiotic formulations in order to achieve intended applicability and effectiveness in therapy. In addition, an innovative and effective strategy is highly encouraged in order to efficiently deliver antibiotics to the target site, optimizing antibiotic usage without affecting the systemic circulation [36].

Table 1. Beneficial aspects of nasal route administration for antibiotic delivery [37]

No	Aspect	Advantages
1	Delivery access	Can be used for local- or systemic therapy and brain targetting (CNS)
2	Bioavailability	Higher than oral administration (avoid hepatic metabolism)
3	Doses	The doses is lower than oral doses
4	Frequency of use	Reduced frequency (can be prolong drug release profile)
5	Systemic side effects	Can be avoid (side effect due to oral administration such as nausea, diarrhea, rash, etc)
6	Chance to resistance	Minimized the threat of resistance
7	Patients compliance	Easy to administer; non-invasive technique

4. MATERIALS AND METHODS

4.1. Materials

Amoxicillin trihydrate (AMT) of analytical grade was obtained from Thermo Fisher (Kandel) GmbH (Karlsruhe, Germany), poloxamer (Kolliphor® P407) was purchased from BASF (Ludwigshafen, Germany), gellan gum (Phytagel®), bovine serum albumin (BSA, lyophilized powder, purity ≥97 %), ethanol 96 % v/v, sodium hyaluronate (NaHa, Mw = 1400 kDa) was donated from Gedeon Richter Plc., mucin from the porcine stomach (Type III), Simulated Nasal Electrolyte Solution (SNES) which consisted of 2.98 g/L potassium chloride (KCl), 8.77 g/L sodium chloride (NaCl), 0.59 g/L anhydrous calcium chloride ($CaCl_2$) dissolved in purified water (pH 5.6), and all reagents were purchased from Merck Ltd. (Budapest, Hungary) if not stated otherwise. Methanol of analytical grade was purchased from Molar Chemicals (Budapest, Hungary). Purified water was filtered using Gradient Water Purification System, the Millipore Milli-Q® (Merck Ltd., Budapest, Hungary). All the other solvents and reagents were of pharmaceutical grade.

4.2. Optimization of albumin-based nanoparticles as nanocarrier system

4.2.1 Factorial design

The preparation of albumin-based nanoparticles was optimized using a 3-factor with 3-level full factorial design in nine independent experiments. TIBCO Statistica® 13.4 (Statsoft Hungary, Budapest, Hungary) software was utilized to generate the design of experiment. The amount of BSA 20% *w/v* (x_1), ethanol (x_2), and purified water (PW) (x_3) was selected as the independent variable and the effect was observed at low, medium, and high levels as depicted in Table 2. In this experiment, the concentration of BSA solution used was 20% *w/v* in order to ensure enough BSA concentration for the formation of intermolecular secondary structure (β-sheet) [38]. Also, the utilized amount of BSA solution and ethanol was considered as critical parameter in the BSA nanogelation process, which is 3 mM of BSA with a minimum of 0.4 mL of ethanol [38,39]. Therefore, the amount of those variables was chosen to be within the above-mentioned concentration, along with the necessity of PW to perform the gelation process. In brief, the BSA 20% *w/v* solution was set from 0.5 to 1.5 mL, while the content of ethanol ranged from 0.6 to 1.2 mL, and the amount of PW was 0.1 to 0.9 mL. Moreover, the design of experiment was employed to investigate the quadratic response surface and to calculate the relationship between variables using the following second-order polynomial model:

$$Y = \beta_0 + \beta_1 x_1 + \beta_{11} x_1^2 + \beta_2 x_2 + \beta_{22} x_2^2 + \beta_3 x_3 + \beta_{33} x_3^2 \quad (1)$$

where Y is the response variable; β_0 is a constant; β_1, β_2, and β_3 are linear coefficients; β_{11}, β_{22}, and β_{33} are quadratic coefficients; x_{1-3} are the main effect factors; and x_1^2, x_2^2, and x_3^2 are the quadratic effect factors. The effect of factors on dependent variables (Z-Average, PdI, and ZP) at 25 °C was presented statistically as the response surface model and analysis of variance (ANOVA) with a 95% confidence interval level, and the variable was considered significant if the $p < 0.05$.

Table 2. Design of experiment for albumin-based nanoparticles optimization. The selected independent variables with the 3-level (−1, 0 and +1) investigated values.

Factors	Level		
	-1	**0**	**+1**
BSA 20% w/v (mL)	0.5	1.0	1.5
Ethanol (mL)	0.6	0.9	1.2
PW (mL)	0.1	0.5	0.9

4.2.2 Preparation of albumin-based nanoparticles

Albumin-based nanoparticles was prepared using desolvating method [40–42] with the composition ratio according to the experimental design results. Briefly, a specified amount of BSA 20% w/v (0.5–1.5 mL) was added into purified water (0.1–0.9 mL) under constant stirring (500 rpm, 37 °C). Then, a certain amount of ethanol (0.6–1.2 mL) was added dropwise. After that, the mixture was homogenized with constant stirring (500 rpm, 37 °C) using a hot-plate magnetic stirrer until the gelation process finished, in which the formation of a high viscosity solution, a bluish-soft gel, and a hard gel can be observed for each formulation. Afterwards, all obtained BSA-based nanoparticles (BSA-NPs) were transferred into vials and then lyophilized using a freeze-dryer (ScanVac CoolSafe, LaboGene, Lynge, Denmark) for 16 hours (at −40 °C, 0.013 mbar pressure), and then continued with secondary drying for four hours at 25 °C. Subsequently, all of the freeze-dried cakes were stored in the fridge at 4 °C for further analysis, and immediately reconstituted with specific amount of purified water prior to each investigation.

4.3. Charaterization of BSA-NPs

4.3.1. Dynamic light scattering measurement

The measurement of the Z-average, PdI, and ZP (ζ) of the reconstituted BSA-NPs was carried out via the dynamic light scattering (DLS) method, using a Malvern Zetasizer Nano ZS (Malvern Instruments, Worcestershire, UK) instrument. All the freeze-dried cakes of BSA-NPs were redispersed with 1.5 mL of PW and stored in folded capillary cells at 25 ◦C. All measurements were carried out in triplicate (n = 3) and the results were expressed as the average ± SD.

4.3.2. Raman spectroscopy

A Thermo Fisher DXR dispersive Raman microscope (Thermo Fisher Scientific Inc., Waltham, MA, USA) was utilized to assess the changes in the secondary protein structure of BSA-NPs after gelation process at the preparation step. The instrument was equipped with a CCD camera and a diode laser running at a 780 nm wavelength, with a laser power of 12 mW and a 50 µm slit aperture size. The obtained spectrum was recorded within a 2-second exposure time and a 6-second acquisition time, collecting a total of 32 scans per spectrum in the spectral range of 3300–200 cm^{-1}, including the cosmic ray and fluorescence corrections.

4.3.3. Thermal gravimetry

The TG investigationwas performed with aMETTLER-Toledo TGA/DSC 1 (Mettler-Toledo GmbH, Gießen, Germany) instrument. Samples of approximately 10 mg were measured into 100 µL aluminum pans, which were then crimped and inserted into the furnace. The experiment was conducted in the temperature range of 25 to 275 °C, with a 10 °C/min heating rate, under a constant nitrogen flow of 50 mL/min. The results were evaluated using the STARe software version 9.00.

4.3.4. Differential Scanning Calorimetry

The DSC examinations were conducted using a Mettler-Toledo DSC 1 (Mettler-Toledo GmbH, Gießen, Germany) instrument at a temperature interval of 25 to 275 °C, with a heating rate of 10 °C/min, under a constant argon flow of 150 mL/min. For the experiments, approximately 5 mg of the samples were measured into 40 µL aluminum pans. Each measurement was normalized to the sample size. The results were evaluated using the STARe software version 9.00.

4.4. Preparation of AMT-loaded BSA-NPs

The preparation of AMT-loaded BSA-NPs were carried out through desolvating method with slight modification [40]. Briefly, 5 mg of AMT was dissolved in 0.9 mL of purified water. After that, 0.5 mL bovine serum albumin solution (20 % w/v) was added into the solution with constant stirring (500 rpm, 37 °C) until clear solutions were observed. Subsequently, 0.8 mL ethanol 96 % v/v was added to the solutions. The mixture was homogenized and heated at 40 °C till a bluish-soft gel formed. Afterwards, glucose 8 % w/v was added into the mixture as a crosslinker agent for stabilizing the resulting AMT-BSA-NPs [42].

4.5. Entrapment efficiency and drug loading capacity of AMT-BSA-NPs

The measurement of entrapment efficiency (%EE) and drug loading capacity (%DL) were performed by adding 1 mL ethanol into 0.5 mL sample of AMT-loaded BSA nanoparticles, and then the mixture was centrifuged using Hermle Z323K high performance refrigerated centrifuge (Hermle

AG, Gossheim, Germany) at 16.000 rpm for 15 min (4 °C). After that, the amount of free AMT in the supernatant was determined using high performance liquid chromatography. The entrapment efficiency (%EE) and drug loading (%DL) capacity were calculated using the following equations [43,44].

$$\%EE = \frac{Initial\ amount\ of\ AMT - Free\ AMT}{Initial\ amount\ of\ AMT}\ x\ 100 \qquad (2)$$

$$\%DL = \frac{Initial\ amount\ of\ AMT - Free\ AMT}{Amount\ of\ BSA\ Nanoparticles}\ x\ 100 \qquad (3)$$

4.6. Development of in situ gelling nasal AMT formulation

4.6.1. Development of in situ thermo-responsive nasal gel of AMT

In this work, the concentration of P407 solution as thermo-responsive polymer was used in a range of 21-25% w/v according to our preliminary studies regarding the suitable concentration for nasal application. Briefly, a certain amount of concentrated P407 solution in purified water which previously prepared overnight (4 °C) was added into the liquid formulation of AMT-BSA-NPs, resulting in various concentration of P407 (21–25% w/v). Finally, the solution was transferred to vials and lyophilized using a freeze-dryer (ScanVac CoolSafe, LaboGene, Lynge, Denmark) at −40 °C for 12 h under a 0.013 mbar pressure, with additional secondary drying at 25 °C for three hours. Freeze-dried formulations were stored in the fridge (4 °C) for further investigations. Each formulation was immediately redispersed with certain amount of purified water prior to each analysis.

4.6.2. Determination of critical ionic concentration of GG as ionic-sensitive polymer

The critical ionic concentration (CIC) is a crucial parameter for the *in situ* ionic-sensitive gelling systems. Firstly, gellan gum (GG) solution in purified water with different concentrations (0.1 %–0.6 %, w/v) were prepared in vials and mixed with various amount (0.1–1 mL) of simulated nasal electro-lyte solution (SNES), which consisted of 8.77 g/L sodium chloride (NaCl), 0.59 g/L anhydrous calcium chloride ($CaCl_2$), and 2.98 g/L potassium chloride (KCl) dissolved in purified water (pH 5.6), with volume ratio between GG solution and SNES as shown in Table 4. Then, after 20 s, the vials were observed for its gelation capacity. Appropriate gel matrix was determine based on visual examination in which the formed gels was able to adhere to the bottom of the vials instead of slipping or flowing down the side [45–48].

4.6.3. Preparation of in situ ionic-sensitive nasal gel of AMT

In this step, the concentration of GG was selected based on our preliminary experimental results of its CIC properties. Briefly, an accurately weighed amount of GG was dispersed in purified water by heating at 90 °C for 30 mins [49] and then cooled to room temperature. Subsequently, the prepared solution of AMT-BSA-NPs was added slowly into the obtained GG dispersion with various concentration (0.2, 0.3, 0.4 % w/v), and the volume ratio was 1:1.5. Finally, the formed *in situ* ionic-sensitive nasal gel of AMT was then lyophilized using ScanVac CoolSafe laboratory freeze-dryer (Labogene, Lynge, Denmark) under 0.013 mbar pressure (−40 °C) for 12 h with an additional secondary drying for 3 h (25 °C). All freeze-dried samples were placed at 4 °C until further investigations. Moreover, prior to each analysis, the freeze-dried samples were immediately redispersed with a specific amount of purified water.

4.7. Characterization of in situ gelling nasal AMT formulation

4.7.1. Particle size, PdI, ZP, pH and osmolality

The particle size, polydispersity index (PdI), and zeta potential of the *in situ* gelling nasal AMT formulations were investigated as described previously. The evaluation of the pH was carried out with pH tester instrument (WTW®inoLab pH 7110, Thermo Fisher Scientific, Budapest, Hungary). Following the pH measurement, the prepared formulations were then characterized for the osmolality by osmometer (Freezing Point Osmometer, Knauer, Berlin, Germany) [33]. All evaluations were conducted in triplicate (n = 3) and data are shown as means ± SD.

4.7.2. Determination of expansion coefficient

Expansion coefficient measurement was carried out according to the previous studies [46,47]. Firstly, 1 mL of each *in situ* gel formulation was mixed with 0.25 mL SNES (pH 5.6) in a graduated test tube and the total liquid volume (V_1) was noted (1.25 mL). Subsequently, the volume of the gel after *in situ* transformation process (V_g) was calculated by the addition of 2.0 mL of SNES and the observed volume was considered as the total volume (V_t); therefore, basically, $V_g = V_t - 2$. The expansion coefficient value (S) was determined based on the following equation [46]:

$$S(\%) = \frac{(V_g - V_1)}{V_1} \times 100 \qquad (4)$$

4.7.3. Determination of water holding capacity

Water holding properties of the *in situ* gelling nasal AMT formulations were calculated following the previous method [45–47]. Approximately 0.25 mL SNES was added into 1.0 mL of

each formulation of the *in situ* gelling formulations in a pre-weighed centrifuge tube. The weight of the gel was noted as W_1. Afterward, the samples were centrifuged at 8000g (10 min, 4 °C) and the formed supernatant was absorbed from the gel using filter paper; the remaining sample (W_2) were weighed. The water holding capacity was measured as the following equation [50]:

$$Water\ holding\ capacity(\%) = \frac{W_2}{W_1} \times\ 100 \qquad (5)$$

4.7.4. Rheological studies

The rheological evaluations of the *in situ* gelling nasal AMT formulations were conducted using a rheometer (Anton Paar Physica MCR302 Rheometer, Anton Paar, Graz, Austria) [38]. The measuring instrument consisted of a cone and plate apparatus with a 1° cone angle. The cone had a diameter of 25 mm and a gap height of 0.05 mm at its center. In case of *in situ* ionic-sensitive nasal gel of AMT (GG matrix) frequency sweep measurements were applied where the storage modulus value (G′) and the loss modulus value (G″) were recorded at 35 °C, over the angular frequency range (0.1–100 rad/s) 0.1 % strain value (which was within the linear viscoelastic region of the systems).

Moreover, in case of the *in situ* thermo-responsive nasal gel of AMT (P407 matrix), the samples were placed at 5 ± 1 °C before measurement. The gelation temperature was recorded as the temperature was raised from 20 to 40 °C with a heating rate of 1 °C/min. At a constant angular frequency of 10 rad/s, strain values of 1% and at 35 °C, the gelation time of the thermos-responsive in situ gelling nasal gel was monitored. The G', loss modulus G", and loss factor were calculated over the angular frequency range at 35 °C from 0.1 to 100 rad/s.

4.7.5. Evaluation of mucoadhesive strength

The measurement of mucoadhesive strength of the *in situ* gelling nasal AMT formulations was conducted using tensile tests by TA-XT Plus texture analyzer instrument (Metron Kft, Budapest, Hungary) [33], configured with a load cell of 5 kg and 1 cm cylinder probe. A filter paper (Whatman® qualitative filter paper, Sigma Aldrich Co. Ltd., Budapest, Hungary) was used as a simulated nasal mucosal surface and impregnated with 50 µL of previously prepared mucin dispersion in SNES (8 % w/w). The sample (20 mg) was affixed to the cylinder probe and put in contact with the wetted filter paper. After applying a preload of 2500 mN for 3 min, the cylinder probe was moved upwards at a predetermined rate of 2.5 mm/min to separate the sample from the substrate. After that, the value of maximum detachment force (mucoadhesive force) was measured. The evaluation was performed in triplicate. Aqueous solution of NaHa (0.5 % w/v) was used as a reference system.

4.7.6. Evaluation of mucoadhesive properties

In order to evaluate the mucoadhesive properties of the *in situ* gelling nasal AMT formulations towards nasal mucin, this evaluation step was carried out by two distinct methods: the displacement method and the flow-through method. At first, approximately 100 g of hot solution containing 1% w/v agar with 2% w/v mucin in purified water was casted onto a petri dish (diameter 10 cm) and left to solidify for 12 h at 4 °C. After that, prior to the test, the petri dishes were then stored at 34 °C for 1 h, to equilibrate following experimental condition. Subsequently, 1 ml of each formulation and as reference AMT aqueous solution (1 mg/ ml) were placed on top of the agar-mucin gel. Further, for the displacement methods [51–53], all petri dishes were oriented at a 60° angle, allowing the samples to move downwards (displacement). The displacement distance was measured in centimeters for up to 2 h, with the adhesion potential being inversely proportional to the sample's displacement.

On the other hand, for the flow-through method [54–57], a modified apparatus was utilized. All petri dishes were inclined at a 60° angle, and the flow of the tempered SNES (35 °C) was maintained through a peristaltic pump with a flow rate of 2 mm/min [58,59] to wash off the formulation from the surface of agar-mucin gel. Around 1–1 ml aliquots of the wash-out solution were collected at pre-determine time points (3, 5, 10, 15, 20, and 30 min). Prior to drug content determination with HPLC, aliquots were freeze-dried and dissolved in 100 µl purified water to ensure that the concentration of analyte reached the limit of detection (LOD). The measurements were performed in triplicate and reported as means ± SD.

4.7.7. Drug content measurement

Determination of AMT content in the *in situ* gelling nasal AMT formulations was conducted by diluting 1 mL sample with 10 mL pH 7.4 phosphate-buffered saline (PBS). Afterwards, the mixture was stirred for 1 h and then analyzed using HPLC. This measurement was conducted in triplicate, data were shown as means ± SD.

4.8. Investigation of in vitro drug release

In vitro drug release study was carried out using the dialysis membrane method [60]. For this investigation, 1 mL of AMT solution in water (1 mg/ml) and the formulations of *in situ* gelling nasal AMT formulation with different GG and P407 concentrations (equals to 1 mg/ml of AMT) were placed in a dialysis bag with 12,000–14,000 MW cut-off (Spectra-por®, Spectrum Labs, Sigma Chemical Co., USA). The investigation was conducted with 100 mL of freshly prepared SNES as the dissolution medium at 50 rpm (35 °C ± 0.5). Aliquots of 0.5 mL of the released medium were withdrawn at specific time intervals up to 240 mins (15, 30, 60, 120, and 240 min). The release

amount of AMT from the *in situ* gelling formulation was analyzed using HPLC. This study was carried out in triplicate. Data were presented as means ± SD.

4.9. Quantification of amoxicillin trihydrate via High Performance Liquid Chromatography

The concentration of AMT in the *in situ* gelling nasal AMT formulations was quantified using HPLC (Agilent Infinity1260, Agilent Technologies, Santa Clara, CA, USA). As a stationary phase, a Kinetex® EVO C18 100 Å column with a particle size of 5 µm and 150 mm × 4.6 mm in size (Phenomenex, Torrance, CA, USA) was applied. For the analysis, 10 µL samples were injected and analyzed at 25 °C using mobile phase of 25 mM phosphate buffer (pH 4.6) (A) and methanol (B). Then, the mobile phase was run at a constant flow rate of 1 mL/min, with a 5 min gradient program, starting with 95 % (A) for the first 2 min, after that the flow rate was immediately decreased to 75 % (A) for an additional 2 min, and finally changed back to 95 % (A) for 1 min. The samples were detected at 230 nm using UV–VIS diode array detector. Data were evaluated using Chem-Station B.04.03. Software (Agilent Technologies, Santa Clara, CA, USA). The retention time of AMT was at 2.5 min, while the regression coefficient (R^2) of the calibration was 1.0 in the concentration range of 12.5–1000 µg/mL.

4.10. Investigation of antibacterial activity

The antibacterial studies were conducted following the recommendation of the European Committee On Antimicrobial Susceptibility Testing (EUCAST) [61]. To assess the antibacterial activities, the disk diffusion method and the following five bacterial strains were utilized: *Haemophilus influenzae* (ATCC® 10211), *Staphylococcus aureus* (ATCC® 29213), *Moraxella catarrhalis* (ATCC® 23238), *Streptococcus pyogenes* (ATCC® 19615), and *Streptococcus pneumoniae* (ATCC® 49619). All prepared strains were β-lactams-sensitive bacteria. The investigations were performed for the freshly prepared AMT solution (1 mg/ml) as a positive control, *in situ* nasal gel (0.3 % w/v of GG and 23% *w/v*) without AMT as a negative control, and the three-three formulations of *in situ* gelling nasal AMT formulations (0.2, 0.3, 0.4 % *w/v* of GG and 21, 22, 23% *w/v* of P407). Firstly, the growth medium of Mueller-Hinton (MH) agar plates (Ref. 64884, Bio-Rad, CA, USA) was prepared according to the manufacturer's instructions for the testing of S. aureus. Whilst, for the other species, the growth medium was prepared following the EUCAST guidelines on Mueller-Hinton agar for Fastidious Organisms (MH-F) (Ref. 43901, Biomerieux, France; MH supplemented with 5 % defibrinated horse blood and 20 mg/L -NAD).

In brief, the suspension of each bacterias with a density of 0.5 McFarland was inoculated into the appropriate agar plates. Afterwards, the sterile disks were then immersed in the drug solutions and immediately placed on the agar plates. After the incubation period (24 h) at room temperature,

the obtained inhibitory zones were analyzed using ImageJ software (ImageJ version 1.52r, U.S. National Institutes of Health, Bethesda, MD, USA). Further, the diameter of inhibitory zones was carefully calculated. The investigations were carried out in separate studies of the five bacterial strains with five times replications for each.

4.11. Ex vivo mucosal permeation studies through human nasal tissue

Ex vivo mucosal permeation study was carried out using human nasal mucosa or mucoperiosteum [62]. The experimental protocol was approved by the institutional ethics committee of the University of Szeged (ETT-TUKEB: IV/3880–1/2021/EKU). Nasal mucosa tissue samples were procured during the routine nasal and sinus surgical procedures (septoplasty), performed under either general or local anesthesia. Briefly, a local injection of 1% w/v lidocaine-Tonogen was given to secure the nasal surgical area. Then, the mucosa was elevated from the nasal base using a Cottle elevator or raspatorium. After that, the obtained nasal mucosa tissue was transported from the surgical facility to the laboratory in a maintained condition using a physiological saline solution, and the experiment was immediately performed.

The permeation study was executed employing a modified Side-Bi-Side® type horizontal permeation apparatus as shown in Figure 3 featuring a diffusion surface area of 0.785 cm^2. The nasal mucosa tissue was cut and excised using a surgical scalpel and affixed between the donor and acceptor compartments. The donor medium was 1 ml of AMT solution (1 mg/ml) and *in situ* gelling AMT formulation, diluted with 8 ml of SNES. Conversely, the acceptor compartment was filled with 9.0 ml of PBS (pH 7.4 ± 0.1). Temperature was maintained at 34 ± 2 ◦C using a ThermoHaake C10-P5 heating circulator (Sigma–Aldrich Co., Ltd., Budapest, Hungary) and stirred at 100 rpm continuously. Sequentially, at 60 min, aliquots (150 µL) from the acceptor chamber were withdrawn. Prior to drug content determination with HPLC, aliquots were freeze-dried and dissolved in 75 µl purified water to ensure that the concentration of analyte reached the limit of detection (LOD). The apparent permeability (P_{app}) of AMT across the nasal mucosa at 60 min was quantified using the following equation [8]:

$$P_{app}(cm/s) = \frac{\Delta[C]_A \times V_A}{A \times [C]_D \times \Delta t} \quad (6)$$

where, ($\Delta[C]_A$) is the concentration differential of AMT in the acceptor chamber after the experiment (60 min), VA is the volume of the acceptor chamber (9 ml), A is the surface area of permeability test (0.785 cm^2), ($[C]_D$) is the initial concentration of AMT in the donor compartment at time point zero and t is the incubation time (s).

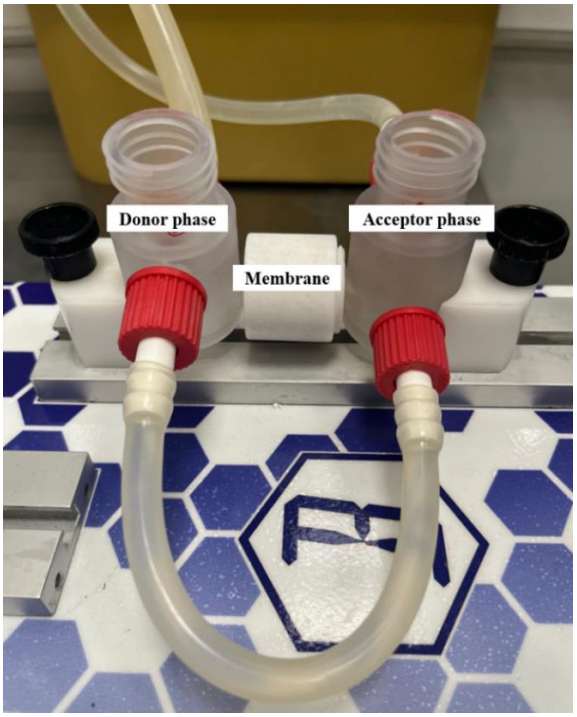

Figure 3. Illustration of Side-Bi-Side® permeation apparatus.

4.12. Ex vivo recovery and extraction assays

The recovery and extraction assays were performed by measuring the amount of AMT retained in the nasal mucosa following the *ex vivo* permeation studies. After completing the *ex vivo* permeation test, the nasal tissue membrane was taken and weighted. Subsequently, the nasal tissue membrane was soaked with 2 ml methanol-water (1:1) and placed on an orbital shaker (PSU-10i Orbital Shaker, Grant Instruments Ltd, Cambs, England) for 60 min at 450 rpm to extract the retained AMT. Prior to AMT content determination with HPLC, aliquots were freeze-dried and dissolved in 100 µl methanol-water (1:1) to ensure that the concentration of analyte reached the limit of detection (LOD).

4.13. Ex vivo retention test by Raman Chemical Mapping

Retention study utilizing Raman chemical mapping was conducted to visually analyze the AMT which retained in the human nasal tissues following the *ex vivo* permeation studies[63]. The nasal tissue membrane was sectioned at 20 microns thickness using microtome (Leica CM1950 Cryostat, Leica Biosystems, Wetzlar, Germany) and put on an aluminum foil-covered glass slide as a sample holder. Raman mapping of cross-sectioned mucosa was carried out utilizing a DXR Raman Microscope (Thermo Fisher Scientific Inc., Waltham, MA, USA), which was outfitted with a charge-coupled device (CCD) camera. Raman maps were acquired from a 100 × 1000 µm surface with a step resolution of 50 µm (60 spectra). This process employed a 780 nm diode laser with an

output power of 12 mW and utilized a 50 μm slit aperture. Each spectral scan was conducted for over 2 s, following a preliminary 2 s laser exposure and the spectrum represented the average of 32 scans within the spectral domain of 3300–200 cm^{-1}. Furthermore, cosmic ray and fluorescence correction were applied in order to decrease the signal-to-noise ratio. The distribution of AMT in the sectioned tissue was determined by using the Raman spectrum of pure AMT as a profile. Raman maps were evaluated through OMNIC 8.3 software (Thermo Fisher Scientific Inc., Waltham, MA, USA).

5. RESULTS AND DISCUSSION

5.1. Optimization of albumin-based nanoparticles

The composition for preparing BSA nanoparticles gel matrices through the gelation process by ethanol-induced method was investigated using a 3-factor with 3-level of full factorial design with 9 standard runs. The ratio of all variables and the obtained responses on the Z-average, PdI, and ZP values are shown in Table 3. Using the TIBCO Statistica 13.4 software, the polynomial equations were created to describe the individual main effects as well as the interaction effects between the independent variables on each dependent variable. Moreover, the Z-average and PdI are the parameters that are highly influenced by the experimental condition. Therefore, the responses of these two parameters were employed for this optimization and their surface plot are shown in Figure 4.

Table 3. Composition of the experimental design with the observed responses. Data are presented as mean ± SD.

Standard run	Independent Variables			Z-average ± SD (nm)	PdI ± SD	ZP ± SD (mV)	Appearance
	BSA 20% (mL)	Et-OH (mL)	PW (mL)				
1	0.5	0.6	0.1	100.63 ± 9.12	0.687 ± 0.16	-32.2 ± 0.64	Hard gel, turbid
2	0.5	0.9	0.9	77.55 ± 0.50	0.409 ± 0.02	-29.7 ± 0.40	High viscosity, bluish
3	0.5	1.2	0.5	81.81 ± 3.68	0.297 ± 0.01	-33 ± 0.60	Hard gel, turbid
4	1.0	0.6	0.9	64.67 ± 2.64	0.326 ± 0.01	-9 ± 0.02	Liquid, clear
5	1.0	0.9	0.5	71.51 ± 13.45	0.584 ± 0.01	-19.2 ± 0.37	Hard gel, turbid
6	1.0	1.2	0.1	138.60 ± 7.43	0.418 ± 0.01	-29.1 ± 0.35	Hard gel, turbid
7	1.5	0.6	0.5	64.35 ± 6.12	0.404 ± 0.04	-10.8 ± 3.44	Liquid, clear
8	1.5	0.9	0.1	198.70 ± 3.10	0.479 ± 0.01	-31.8 ± 0.45	Hard gel, turbid
9	1.5	1.2	0.9	98.91 ± 5.78	0.675 ± 0.01	-15.6 ± 1.33	Liquid, clear

According to multiple regression analysis on the experimental data, the relationship of the variables on Z-average (Y_1) could be described using the following equation:

$$Z\text{-}average = 99.61 + 16.995x_1 + 14.985x_2 - 22.1x_3 + 12.2325x_2^2 - 27.235x_3^2 - 13.89x_1x_2 + 16.11x_1x_2^2 \quad (7)$$

The regression coefficient of the surface plot was 0.98086 (R^2). Based on the polynomial equation, the positive sign before the variables indicates that the effects of those variables are directly proportional to the Z-average. The increase in the concentration of BSA and ethanol subsequently increases the value of the Z-average. The interaction between BSA and ethanol can encourage

gelation to occur, thus generating the larger particle size of the obtained BSA nanoparticles [40–42,64]. Meanwhile, the negative sign indicates that the effect of the variable is inversely proportional to the Z-average. The increase in purified water results in a reduced particle size of BSA nanoparticles. The reduction of the Z-average value could be due to the ability of purified water to enhance the solubilization of BSA, leading to a lower concentration of BSA in the formulation for performing gelation while in contact with ethanol [38].

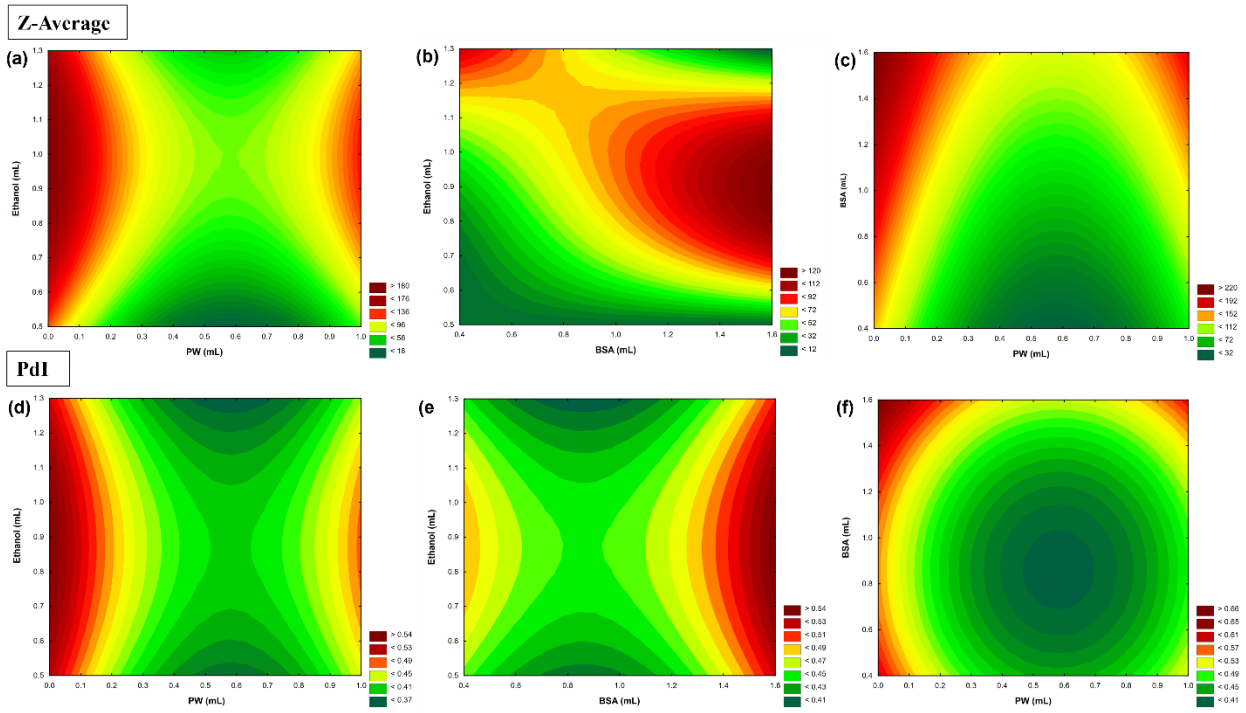

Figure 4. Response surface plots showing the effect of independent variables PW ─ Ethanol (a), BSA ─ Ethanol (b) and PW ─ BSA (c) on Z-average as well as PW ─ Ethanol (d), BSA ─ Ethanol (e) and PW ─ BSA (f) on PdI.

Furthermore, the effect of the independent variables on PdI (Y_2) can be described with the following equation:

$$PdI = 0.475444 + 0.0275x_1 - 0.029x_3 - 0.024583x_1^2 + 0.011417x_2^2 + 0.094583x_3^2 + 0.259833x_1x_2 \quad (8)$$

The regression coefficient (R^2) of the surface plot was 0.98228. It was found that the amount of water (x_3) and the interactive influence of BSA and ethanol (x_1x_2) demonstrated a significant effect on the PdI. The coefficients with positive signs indicate the directly proportional relationship of the variable with the PdI, which means that a higher amount of the variable can lead to a higher PdI value in the resulting formulation. The higher PdI value can be explained as being due to the increased concentration of BSA affecting the tendency of the particles to form aggregates [65].

Moreover, the negative sign of the coefficients indicates that the effect of the variables is inversely proportional to the PdI, in which the addition of those variables might decrease the PdI value. The amount of purified water influences the concentration of BSA in the formulation, in terms of the ability to solubilize BSA, resulting in a reduced aggregation of the particle and generating a lower PdI value [65].

5.2. Structural investigation of BSA-NPs

5.2.1. Raman spectroscopy

The addition of ethanol to the BSA solution by up to 30% v/v can cause the unfolding of albumin, indicating a change in the α-helical structure. Therefore, Raman spectroscopic studies were performed (Figure 5) to investigate the refolding behavior of BSA-NPs after the removal of ethanol through the freeze-drying process. The intensity changes of the peak at 1655 cm^{-1} (amide I region) in the Raman spectra of BSA, which can usually be attributed to the ordered α-helix (ho), indicate the unfolding and refolding of the protein. In the Raman spectrum of BSA-EtOH, the decreased intensity of the amide I peak suggests the unfolding of BSA [66], while the peaks appearing at 882 cm^{-1} (CCO skeleton symmetric stretching vibration), 1047 cm^{-1} (CO scaling), 1088 cm^{-1} (CCO skeleton stretching vibration), 1279 cm^{-1} (CH_2 deformation), and 1456 cm^{-1} (CH_3 antisymmetric deformation) are characteristic of ethanol [67]. These characteristic peaks cannot be identified in the spectrum of the BSA nanoparticles, indicating a successful freeze-drying process, while the increased intensity of the amide I peak in comparison to BSA-EtOH supports the possible partial refolding of BSA after the redispersion of the nanoparticles in purified water, due to hydrophobic interactions.

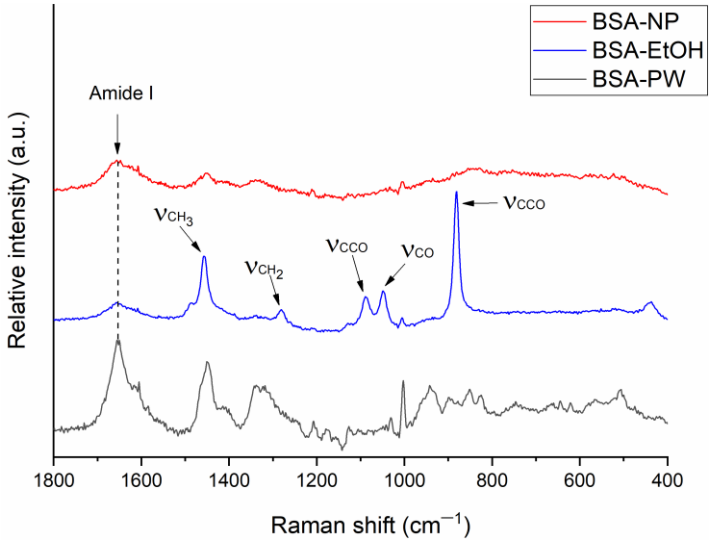

Figure 5. Raman spectrum of the BSA aqueous solution (BSA-PW), BSA nanoparticles after being desolvated with ethanol (BSA-EtOH), and BSA nanoparticles after the freeze-drying process (BSA-NP).

5.2.2. TG analysis

TG analysis was performed to determine the residual ethanol content and support the Raman investigations. The TG thermograms as shown in Figure 6 revealed that BSA undergoes denaturation above 60 °C, as indicated by the weight loss. Ethanol evaporates within the same temperature range (45–110 °C); therefore, we investigated the weight loss in the mentioned temperature interval and compared it with the TG curve of the initial BSA. As ethanol belongs to the Class 3 solvents, its residual concentration should be less than 5000 ppm in a daily dose of the final product, a requirement of the International Conference for Harmonization (ICH) Q3C (R5) guidelines for residual solvents [68]. It has been revealed that, when comparing the weight loss of BSA-NPs formulations to the initial BSA, no remarkable difference was obtained, indicating that the residual ethanol content is under the limit of detection, thereby meeting the acceptance criteria of the ICH (Table 4).

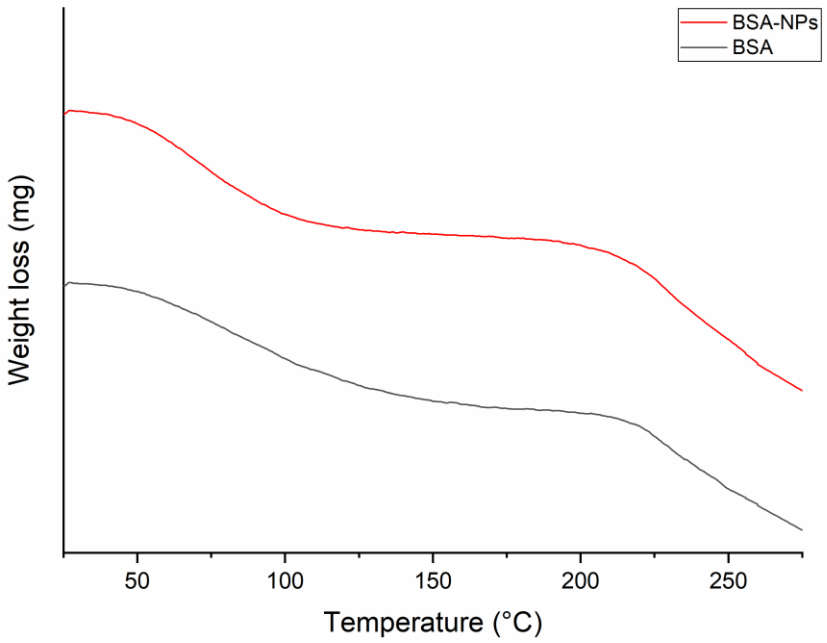

Figure 6. TG curve of BSA nanoparticles after the freeze-drying process (BSA-NPs) compared to the initial BSA.

Table 4. Weight-loss results for the BSA-NPs formulation in comparison to the initial BSA

Formulation	Weight Loss (mg)	Weight Loss (%)
Initial BSA	0.2507	6.67
BSA-NPs	0.2515	6.69

5.2.3. DSC

DSC study was conducted in order to further investigate the thermal behavior of BSA-NPs formulations. In accordance with the TG results, the endothermic peak at 91 °C that was seen in the DSC thermogram (Figure 7) of the initial BSA indicates the denaturation temperature of protein, while the endothermic peak at approximately 217 °C belongs to its melting point [69]. In the case of BSA-NPs, the denaturation peak of BSA was markedly shifted to a lower temperature proportional to the BSA content of formulations [70]. However, the melting point of BSA increased in all BSA-NPs formulations, supporting the formation of nanoparticle complex.

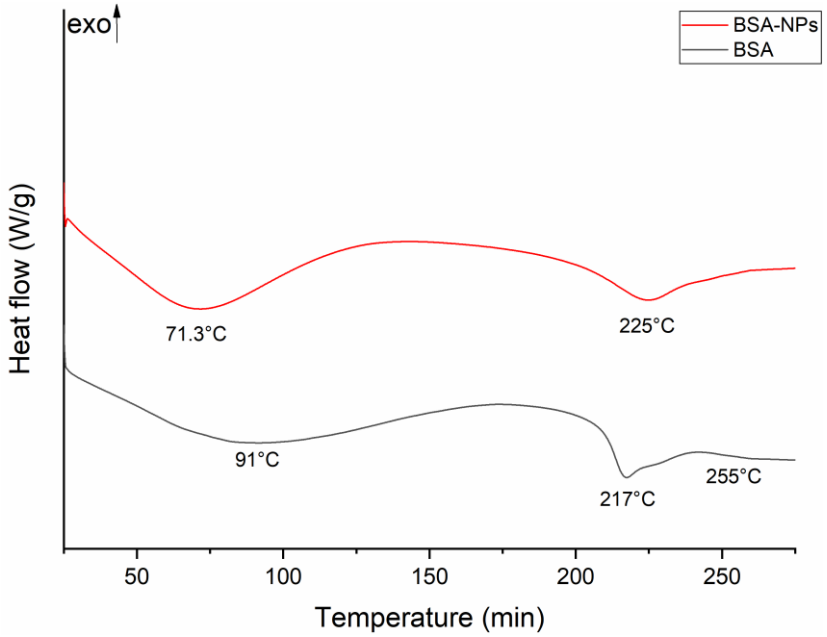

Figure 7. DSC thermogram of BSA nanoparticles after the freeze-drying process (BSA-NPs) compared to the pure BSA.

5.3. Entrapment efficiency and drug loading capacity of AMT-BSA nanoparticles

Entrapment efficiency (*%EE*) and drug loading (*%DL*) capacity of AMT-loaded albumin nanoparticles was observed to be 95.62 ± 0.07% and 2.18 ± 0.01%, respectively. The high entrapment efficiency of albumin nanoparticles could be attributed due to the high binding capacities of albumin, in which the presence of positively and negatively charged amino acids in bovine serum albumin allows the interaction with various hydrophilic or lipophilic drugs [71,72]. Whereas, a small drug loading capacity might be due to a low amount of AMT used in the formulation with a quite high concentration of BSA solution (20% w/v), in order to ensure all AMT is properly loaded into the nanoparticles

5.4. Determination of critical ionic concentration of gellan gum

The GG solutions can undergo a sol-gel transformation upon contact with SNES following nasal administration [34]. Therefore, the range of GG concentration was investigated based on the minimum concentration of SNES required to produce gelation with acceptable viscosity for nasal application [73]. According to our preliminary studies regarding the appropriate ratio between GG solution in water and SNES using Rheometer, it was found that the storage modulus (G') reached its maximum in the ratio of 2:1 *v/v* (water:SNES) and will not further increase even though in case of applying a higher ratio of SNES. Therefore, the 2:1 *v/v* ratio of water:SNES was considered as the maximum ratio to be used in determining the critical ionic concentration of GG.

As shown in Table 5, the results showed that cation concentrations in SNES were subcritical, and GG solutions with a concentration of more than 0.3% *w/v* might rapidly transform into a clear, colorless gel. Accordingly, the greater the concentration of GG, the more sensitive it is to experience the sol-gel transition. This indicated that the correlation between the GG concentration and gelation characteristics was directly proportional [29]. However, the increased viscosity of GG at the higher concentration rendered administration in the nasal cavity inconvenient. Thus, the concentration of GG below 0.5% *w/v* was considered ideal to employ in the *in situ* ionic-sensitive nasal gel of AMT formulation. In addition, considering the influence of BSA in the formulation, which can affect the gelling properties of the *in situ* ionic-sensitive nasal gel, then GG solution with a range concentration of 0.2 – 0.4% *w/v* was chosen for preparation and further investigation

Table 5. Gelation properties based on the ratio between GG and SNES

GG concentration	**Ratio of GG:SNES (*v/v*)**				
(% *w/v*)	**2:0.1**	**2:0.2**	**2:0.5**	**2:0.8**	**2:1**
0.1	-	-	-	-	-
0.2	-	-	-	±	±
0.3	-	-	±	±	+
0.4	-	±	±	+	+
0.5	+	+	+	+	+
0.6	+	+	+	+	+

5.5. Characterization of in situ gelling nasal AMT formulation

5.5.1. Particle size, PdI, ZP, pH, and osmolality

The measurement of Z-average, PdI, and ZP was carried out to characterize the *in situ* gelling nasal AMT formulation since these variables could have an impact on nasal mucosal

absorption. Overall, the results in Table 6 showed that the Z-average value of all *in situ* gelling AMT formulations complied with the recommended size for optimal applicability for nasal administration, which should be within 200 nm [74] to maximize the surface area of the formulation to be in contact with nasal mucosa. However, particle size of the *in situ* thermo-sensitive nasal gel of AMT formulation (P21%, P22%, and P23%) were slightly higher compared to the *in situ* ionic-sensitive nasal gel of AMT formulation (GG0.2%, GG0.3%, and GG0.4%). In term of this, it has been previously studied that a significant interaction might occur between the smaller nanoparticles and bacterial membrane [75]. Smaller nanoparticles can have stronger antibacterial action because of their increased surface area for interacting and binding with bacterial surfaces and their ease of penetration into bacterial membranes [76,77]. Moreover, for the zeta potential results, negative surface charges were observed for all *in situ* gelling AMT formulations. In line with this, since the nasal mucosa also has a negative charge due to the ionic composition of the mucus [78], hence repulsive interactions can occur and nasal absorption of the *in situ* gelling AMT formulation may perform in a low tendency [79]. Thus, these characteristics may provide greater benefit for local nasal delivery. Additionally, for the PdI results, all *in situ* gelling AMT formulation showed a quite similar value.

Furthermore, the pH of all *in situ* gelling AMT formulation was also evaluated since it can influence patient comfort following the administration into the nasal cavity. Besides that, the pH of nasal preparation can predominantly affect the frequency of ciliary beat [80]. According to the results, the pH values of all *in situ* gelling AMT formulations exhibited quite similar results, which suitable for nasal administration. in this case, the pH of human nasal mucosa ranges around 5.5 to 6.5 [81,82], with a baseline nasal pH of about 6.3 [83]. Nevertheless, the pH values are frequently altered in disease states, for instance, patients with rhinosinusitis typically have nasal pH values between 5.3 and 7.6 [84]. Subsequently, with regards to the rhinosinusitis treatment, the tonicity of nasal product is also essential to investigate. Based on the results of osmolality measurement, all *in situ* gelling AMT formulations demonstrated a hypertonic condition, in which a quite higher value was observed for the *in situ* thermo-sensitive formulations (P21%, P22%, and P23%) compared to the *in situ* ionic-sensitive formulation (GG0.2%, GG0.3%, and GG0,4%). Interestingly, for the treatment of rhinosinusitis, the hypertonic solution was found to be well-tolerated and more efficacious in comparison to the isotonic solution or normal saline [85–89]. Also, the hypertonic solution showed higher clinical benefits, including minimizing adverse effects, reducing related symptoms, and improving patient's quality of life in terms of sinus-state [85,86,88,90].

Table 6. Z-average, PdI, ZP, pH, and osmolality of *in situ* gelling AMT (Means ± SD, n = 3).

***In situ* gelling formulation**	**Z-average ± SD (nm)**	**PdI ± SD**	**Zeta potential ± SD (mV)**	**pH ± SD**	**Osmolality ± SD (mOsm/kg)**
P21%	118.43 ± 3.02	0.615 ± 0.02	−18.43 ± 0.3	6.74 ± 0.01	663 ± 2
P22%	134.53 ± 2.90	0.648 ± 0.03	−18.67 ± 0.1	6.89 ± 0.01	623 ± 3
P23%	137.20 ± 2.66	0.682 ± 0.01	−19.76 ± 0.5	6.86 ± 0.01	611 ± 2
GG0.2%	46.50 ± 2.34	0.592 ± 0.03	−22.8 ± 0.2	6.61 ± 0.01	460 ± 2
GG0.3%	65.90 ± 2.78	0.504 ± 0.01	−22.7 ± 0.3	6.51 ± 0.01	493 ± 2
GG0.4%	83.34 ± 3.08	0.615 ± 0.02	−33.2 ± 0.1	6.25 ± 0.01	557 ± 1

5.5.2. Expansion coefficient

The transformation (solution–gel systems) of *in situ* gelling formulation will definitely increase the volume of the instilled dosage form once in contact with particular conditions in the nasal cavity. Thus, it might form a clog in the nasal passage and create physical discomfort for the patient due to its larger dimension [91]. Therefore, it is important to investigate the expansion coefficient of the *in situ* gelling of AMT formulation. According to the result in Figure 8, overall, the findings showed that no overt volume growth was observed. However, the expansion coefficient of the *in situ* thermo-sensitive formulation (P21%, P22%, and P23%) was found higher (5.3−12.6%) compared to the *in situ* ionic-sensitive formulation (GG0.2%, GG0.3%, and GG0.4%) with around 3.7−8.2%. In this case, a smaller value may seems convenient with a proper transition of solution-gel, thus patients would not experience any substantial discomfort when the formulation was applied to the nasal cavity.

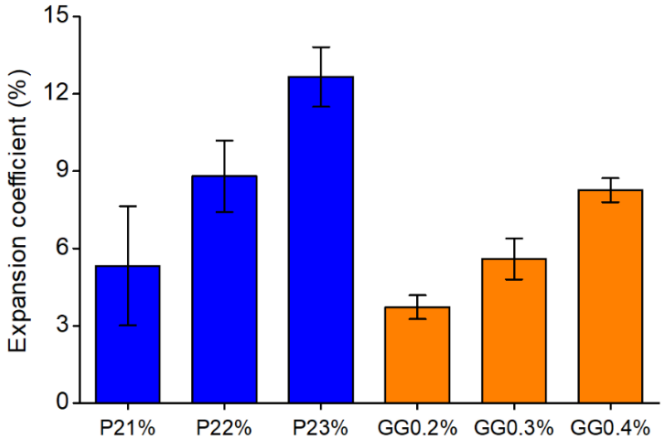

Figure 8. Expansion coefficient of all *in situ* gelling AMT formulation. Data are shown as means ± SD, *n* = 3.

5.5.3. Water holding capacity

The *in situ* gelling formulation should be capable of hydrating and holding water to provide optimal mucoadhesive behavior. In this case, the water holding capacity was related to the texture properties of the produced nasal gel [50]. Higher water holding capacity may indicate a more elastic gel properties than brittle gels. Also, sufficient water holding capacity can ensure better humidity in the nasal mucosal, which might contribute to facilitating drug absorption [92].

In this study, the measurement was conducted for both type of formulations; the *in situ* thermo-sensitive and the *in-situ* ionic-sensitive. However, in case of the *in situ* thermo-sensitive formulation (P21%, P22%, and P23%), no changes was observed after the evaluation. At the end, the mixture of formulation and SNES was still in a liquid state, which might be due to the addition of SNES into the formulation, reducing the concentration of polymer (P407) in total solution. Consequently, the ability to transform solution to gel was also reduced. Meanwhile, for the *in situ* ionic-sensitive formulation (GG0.2%, GG0.3%, and GG0.4%), the results in Figure 9 showed that the values of water holding capacity were in the range of 87.96−90.44% and no significant difference between GG concentration (p>.0.05). This result suggested that the *in situ* ionic-sensitive nasal gel of AMT possess a favorable water holding capacity.

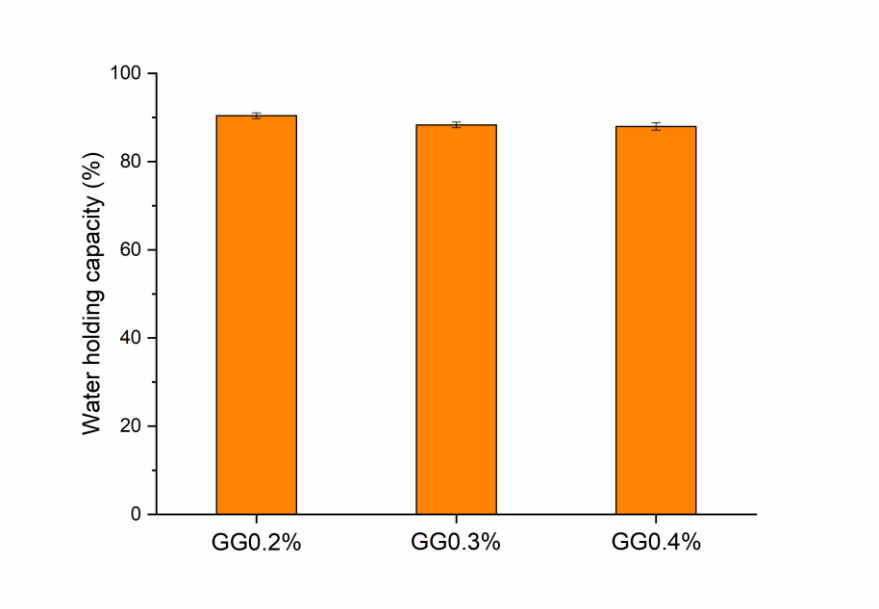

Figure 9. Water holding capacity of *in situ* ionic-sensitive nasal gel of AMT. Data are shown as means ± SD, n = 3.

5.5.4. Rheological studies

The rheological evaluation of *in situ* thermo-sensitive formulation (P407 matrix) were conducted to observe the gelling temperature and gelling time. Gelation temperature ($T_{sol\text{-}gel}$) is one of the critical parameters in formulating the *in situ* gelling thermosensitive nasal gel. The

optimized formulation should remain in liquid form at room temperature to provide the correct dosing and immediately change to a gel form when administered into the nasal cavity due to the nasal physiological temperature [32]. The average temperature in the nasal cavity is reported as ~35°C [25].

In this study, the investigation was conducted using five different concentrations of P407 (21–25% w/v). Based on the results shown in Figure 10, the suitable concentration for gelling temperature and gelling time was in the range of 21−23% *w/v* of P407. The $T_{sol\text{-}gel}$ of 21, 22, and 23% *w/v* P407 were 33.43 ± 1.11°C, 32.11 ± 1.9°C, and 27.71 ± 0.35°C, respectively. These results showed that as the concentration of P407 increases, the $T_{sol\text{-}gel}$ of *in situ* gelling nasal preparations decreases. This phenomenon is basically due to the effect of the P407 concentration. The gelation process is linked to the hydrophilic-hydrophobic structure of P407, which involves dehydration process of the PPO block and then hydration of the PEO block that affects the polymer to swell based on its concentration [93].

Furthermore, the gelling time can be explained as the time required to undergo sol-gel transition at the nasal physiological temperature after administration. The gelling time is critically essential for *in situ* gelling thermosensitive nasal preparation, as it is significantly associated with the bioavailability of the drug. If the gelation process performs too slowly, the product will be easily eliminated from the nasal passage due to mucociliary clearance. However, the rapid gelation process will make it challenging for the product to spread well on the nasal mucosa, which results in a lower absorption surface and affects its efficacy [33,94]. In this study, the investigation revealed that gelling time decreases with an increase in P407 concentration. The obtained values varied (1–3.5 min) for the concentrations of 21, 22, and 23% w/v. These results are evidently suitable for nasal application.

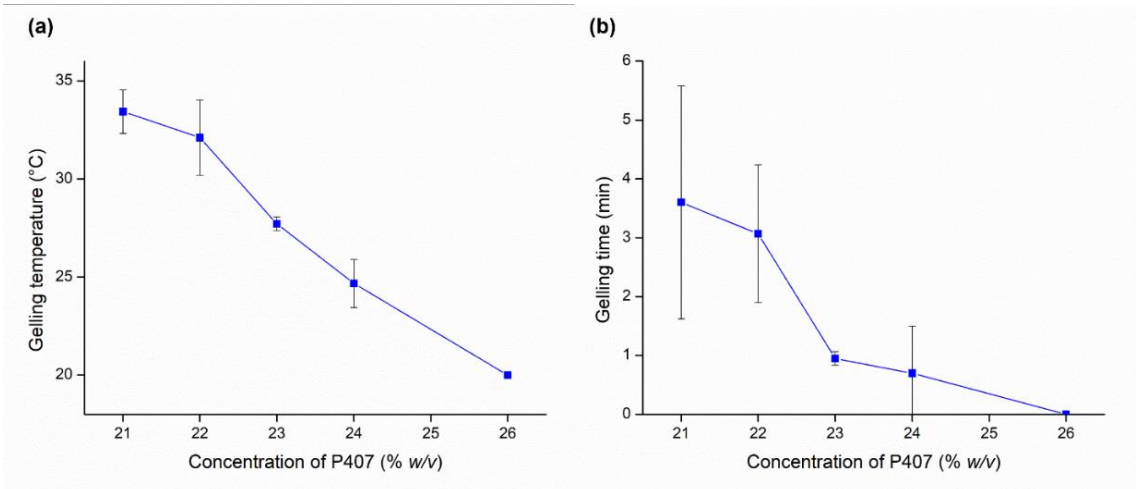

Figure 10. Gelling properties of *in situ* thermo-sensitive formulation. Data are expressed as means ± SD, *n* = 3.

Meanwhile, the results as depicted in Figure 11 showed the storage modulus (G') value of the *in situ* ionic-sensitive nasal gel of AMT formulations (GG0.2%, GG0.3% and GG0.4%) at nasal temperature (35°C). Determination of gel strength of the *in situ* ionic-sensitive nasal gel of AMT were calculated by comparing the storage modulus (G') value at a constant frequency of 1 and 10 rad/s, as this frequency range corresponds to the shear rate of nasal cilia [95]. The G' value represents the elastic behavior, which is described as the stored energy in a solid-state due to the elastic deformation. Therefore, the G' can reflect on the gel strength properties of the formulation. The higher the storage modulus, the greater the gel strength [96]. According to the results, as the GG concentration increased, the G' value increased. Moreover, G′ values of the *in situ* ionic-sensitive nasal gel of AMT were in the range of 750-2500 Pa (with the highest G' value of GG0.4%) indicating proper gel strength behavior for nasal applicability, more permanently resisted to mucociliary clearance.

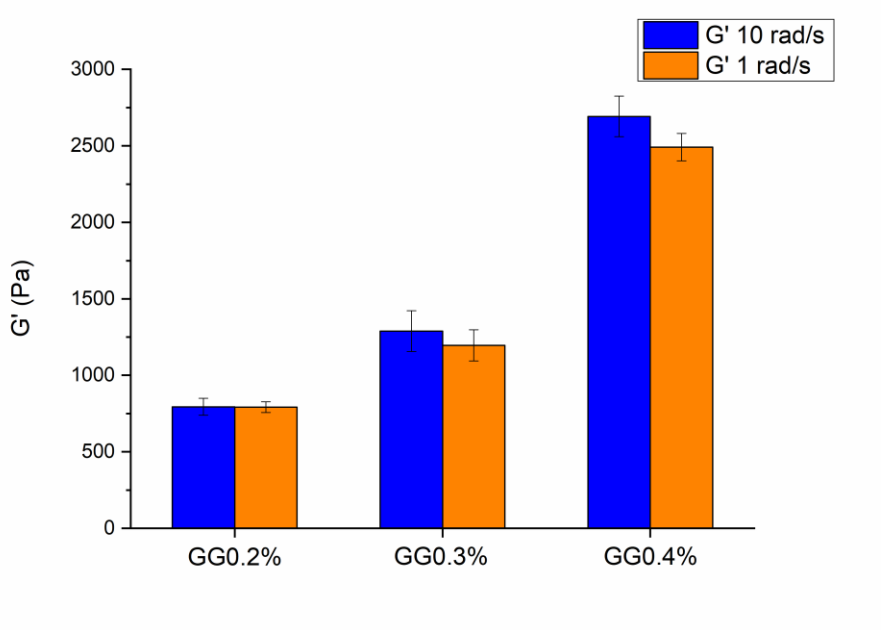

Figure 11. Storage modulus (G') value of the *in situ* ionic-sensitive nasal gel of AMT. Data are expressed as means ± SD, n = 3.

5.5.5. Mucoadhesive strength

Mucoadhesion is a crucial parameter for *in situ* gelling formulation as it can prevents rapid drainage of the gels from the nasal cavity and thus affects the bioavailability [97,98]. Therefore, appropriate mucoadhesive properties are important in terms of illustrating the force of attraction between the *in situ* gelling formulation and the surface of the mucus layer [99]. The presence of the hydrogen bond formation due to the rapid absorption of fluid from the mucus layer (simulated mucosal membrane) could explain the enhancement of the mucoadhesive forces of the *in situ* gelling

formulation [100]. This allows the polymer chains to enter the mucin network and form adhesive bonds. Adhesive force is a detachment force which illustrates the force of attraction between the surface of the mucus layer and the prepared gel [99].

Based on the results shown in figure 12, the adhesive force of the *in situ* thermo-sensitive (P21%, P22%, P23%) were varies within the range of 1400 – 1700 mN. Meanwhile, for the *in situ* ionic-sensitive formulation (GG0.2%, GG0.3%, and GG0.4%), the values were found higher, within 1900 – 2000 mN. Moreover, in comparison to 0.5% w/v solution of NaHa, a well-known and widely used mucoadhesive polymer for ocular and nasal formulations, the formulation of *in situ* ionic-sensitive nasal gel demonstrated a significantly higher adhesive force value ($p < 0.05$). This finding also supports the possibility of a longer residence time of the *in situ* ionic-sensitive nasal gel of AMT formulations on the nasal mucosa following nasal administration compared to the *in situ* thermo-resposnsive formulation.

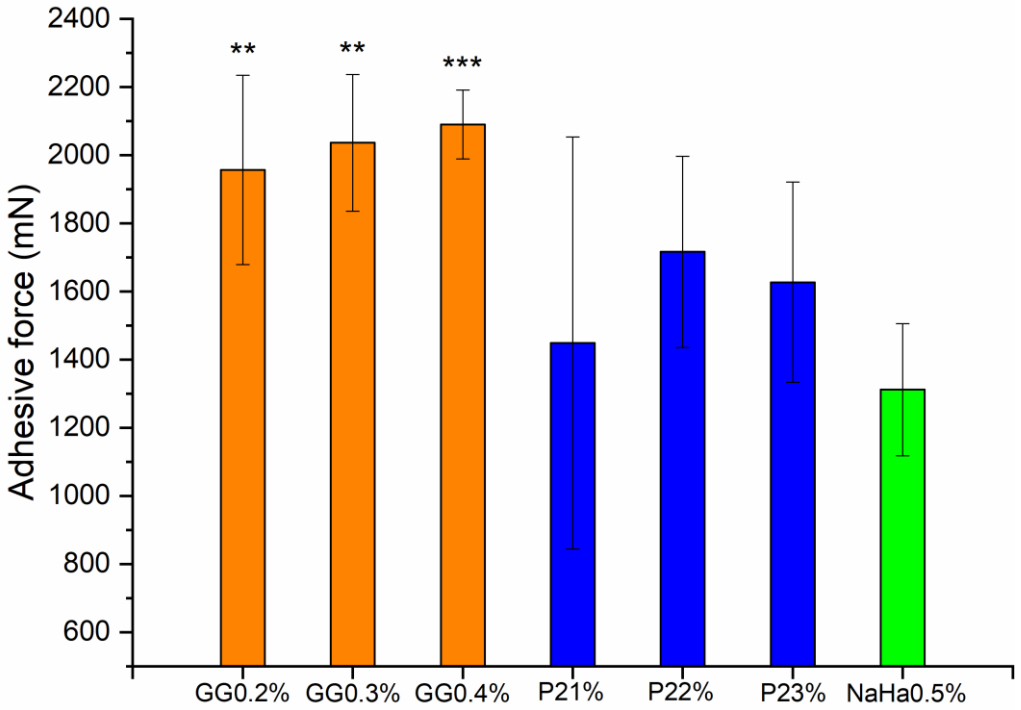

Figure 12. Mucoadhesive strength of the *in situ* gelling nasal formulations of AMT in comparison to 0.5% *w/v* NaHa aqueous solution. Data are presented as means ± SD, $n = 3$. Statistical analysis: Student's *t*-test (** p<0.00, *** p <0.001).

5.5.6. Mucoadhesive properties

The investigation of mucoadhesion properties of the *in situ* gelling AMT formulation was assessed by two modified methods, namely the flow-through and the displacement method. In this work, all *in situ* thermo-sensitive nasal gel of AMT formulation (P21%, P22%, and P23%) was unable to

perform sol-gel transition and cannot attach on the surface of agar-mucin due to its liquid state that made it directly move downward once placed on the surface of the inclined agar-mucin gel. Therefore, the measurement only conducted for the *in situ* ionic-sensitive nasal gel of AMT formulation (GG0.2%, GG0.3%, and GG0.4%).

The results of the flow-through method, as illustrated in Figure 13 showed that the washed amount of AMT from all samples increased by the time. The *in situ* ionic-sensitive nasal gel of AMT formulations (GG0.2%, GG0.3%, and GG0.4%) exhibited a lower washed amount of AMT in comparison to the AMT 1 mg/ml solution. The washed amount of AMT tends to be proportional to the concentration of GG in the formulation. The higher the GG concentration, the lower the amount of AMT obtained after washed off process. This can be explained through the mechanism in which the SNES droplets from peristaltic pump promote ionic condition (providing Ca^{2+}) that immediately facilitate the sol-gel transformation of GG in the formulation, resulting in a higher viscosity solution that is able to be retained on the surface of agar-mucin gel [101]. Moreover, the mucoadhesive properties were also supported by the interaction between the BSA content in the *in situ* gelling formulations of AMT with the mucin in the agar mixture. The BSA plays an important role for the interaction with mucin, due to its high binding affinity to the mucin, which known as BSA-mucin binding [102–104]. Accordingly, the *in situ* gelling AMT formulations can definitely attach to the surface of agar-mucin gel, that indicates high mucoadhesive potential, resulting in a lower amount of washed-out AMT.

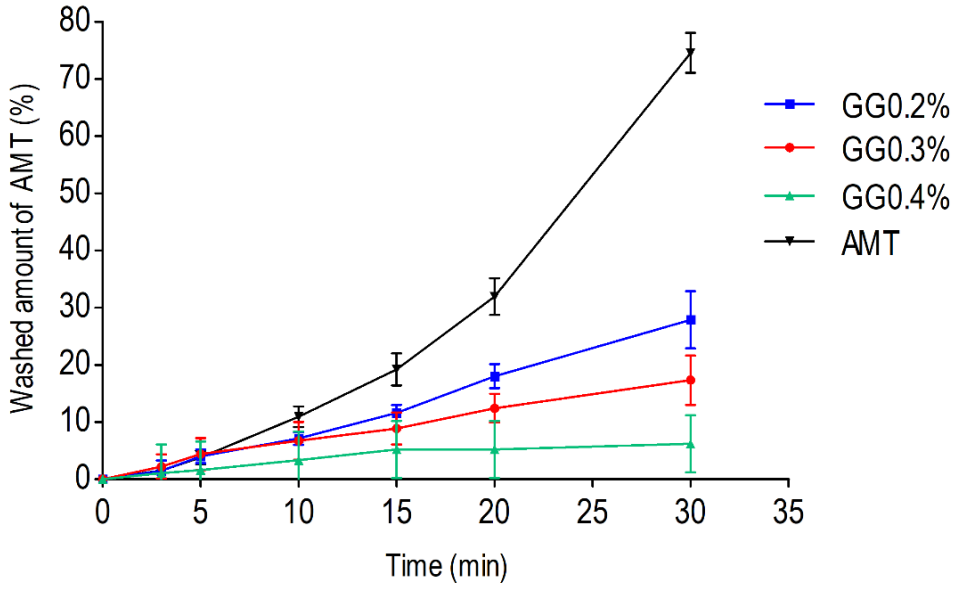

Figure 13. The flow-through method, illustrating the washing resistance of all *in situ* gelling AMT formulations (GG0.2%, GG0.3%, and GG0.4%) in comparison to the AMT solution (1 mg/ml) as control. Data are shown as means ± SD, $n = 3$.

In addition, for the displacement method, the results as shown in Table 7 exhibited a quite similar results with the previously mentioned method. The AMT solution directly moved downward while placed on the surface of inclined agar-mucin gel, due to its behavior as a liquid solution. Meanwhile, the formulations of *in situ* ionic-sensitive nasal gel of AMT formulations showed interesting displacement results for up to 2 h of investigation. The formulation of GG0.2% showed a higher displacement distance of about 5.5 ± 0.2 cm, compared to GG0.3% and GG0.4% with approximately 1.6 ± 0.3 cm and 1.1 ± 0.2 cm, respectively. These results reflect good adherence and recorded as good mucoadhesion potential. Overall, the evaluation of mucoadhesive properties demonstrated that the *in situ* ionic-sensitive nasal gel of AMT formulation (GG0.2%, GG0.3%, and GG0.4%) have the potential to adhere to the nasal wall once instilled to the nasal cavity and would not be easily washed out, allowing the formulation to be retained to the nasal mucosa and release the drug.

Table 7. Displacement distance of the *in situ* ionic-sensitive nasal gel of AMT formulation and AMT solution. Data are shown as means ± SD, $n = 3$.

Formulation	**AMT solution (1 mg/ml)**	**GG0.2%**	**GG0.3%**	**GG0.4%**
Displacement after 2 h (cm)	-*	5.5 ± 0.6	1.6 ± 0.3	1.1 ± 0.8

* Not measurable, directly flows downwards

5.5.7. Determination of drug content

The *in situ* gelling formulations of AMT (GG0.2%, GG0.3%, GG0.4%, P21%, P22% and P23%) theoretically contained AMT equivalent to 1 mg/ml concentration. In this study, the drug content was examined to confirm that enough amount of AMT remained inside the *in situ* gelling formulation and to demonstrate that the preparation has proper solubilization properties that could completely dissolve all of its substances. Drug content percentage of all *in situ* gelling AMT formulation was observed in the range of 98.41–103.15%. This finding demonstrated that the procedure which was used for fabricating the *in situ* gelling nasal formulations of AMT did not cause a reduction in drug amount or loss of drug during formulation process. In addition, the drug content recovery complied with ICH requirements for an acceptable range for analytical procedures [105]. Therefore, it was confirmed that the amount of AMT in the *in situ* gelling AMT formulations was not affected by the fabrication method and the integration of AMT-loaded BSA-NPs into the *in situ* gelling polymers (GG and P407) could produce a proper distribution of drug (AMT) throughout the *in situ* gelling matrix.

5.6. Investigation of in vitro drug release

The investigation of *in vitro* drug release were conducted using the dialysis membrane method [83] in a simulated nasal electrolyte solution (SNES) medium for 240 min at 35 ± 0.5 °C. The i*n vitro* drug release profiles (Figure 14) showed the results of *in situ* thermo-responsive AMT formulation (P21%, P22%, and P23%) as well as the *in situ* ionic-sensitive AMT formulation (GG0.2%, GG0.3%, and GG0.4%) in comparison with the pure drug (AMT 1 mg/ml solution in water). Overall, the release behavior of AMT from the *in situ* gelling AMT formulation demonstrated a controlled drug release profile, which may result due to the influence of the consistency and structure of the obtained nasal gel [106] and sufficient crosslinks in the polymer matrix of BSA nanoparticles that could possibly hinder the release of the drug from the polymer [43,107].

For the results of *in situ* thermo-responsive AMT formulation (P21%, P22%, and P23%), in the first hour, 48.07 ± 2.61% and 49.96 ± 4.35% of drug release were observed for P22% and P23%, followed by 62.92 ± 6.78% of drug release for P21%, compared to pure AMT (control) which has released the drug of 95.68 ± 3.4%. Moreover, after 4 h, 91.37 ± 2.98% of AMT was released from P21%. Meanwhile, for P22% and P23% the release of AMT was 78.53 ± 8.70% and 79.61 ± 6.15%, respectively, and the complete release profile was achieved by pure AMT as the control solution. This findings demonstrated that as the concentration of P407 increased, the viscosity of formulation increased, leading to a tighter structure of the gel, which decreased the release of the drug (prolonged drug release) [33,108]. Moreover, the gel erosion rate as well the drug diffusion rate are the two mechanisms that control the release profile of P407-based nasal gel [93,108].

Furthermore, for the i*n vitro* drug release profiles of the *in situ* ionic-sensitive nasal gel of AMT formulation (GG0.2%, GG0.3%, and GG0.4%) showed that in the first 60 mins around 53.34 ± 3.61%, 45.15 ± 4.35%, and 45.31 ± 6.7% drug release for GG0.2%, GG0.3% and GG0.4%, respectively. Meanwhile, AMT solution (control) showed around 95.68 ± 3.4%. After 240 mins GG0.2%, GG0.3% and GG0.4% exhibited around 89.87 ± 2.98%, 87.41± 8.70%, and 84.43± 6.15% release of AMT, respectively. The GG gel structure once in contact with SNES, appeared more closely packed and coupled with sufficient crosslinked properties through the BSA nanoparticle matrix, thus able to inhibit drug release from the polymer [43]. In addition, as the concentration of GG increased, the viscosity of the formulation also increased. This phenomenon might occur due to the polymer chains becoming closer, resulting in more interactions between molecules leading to a thicker network structure of the prepared nasal gel and decrease the drug release.

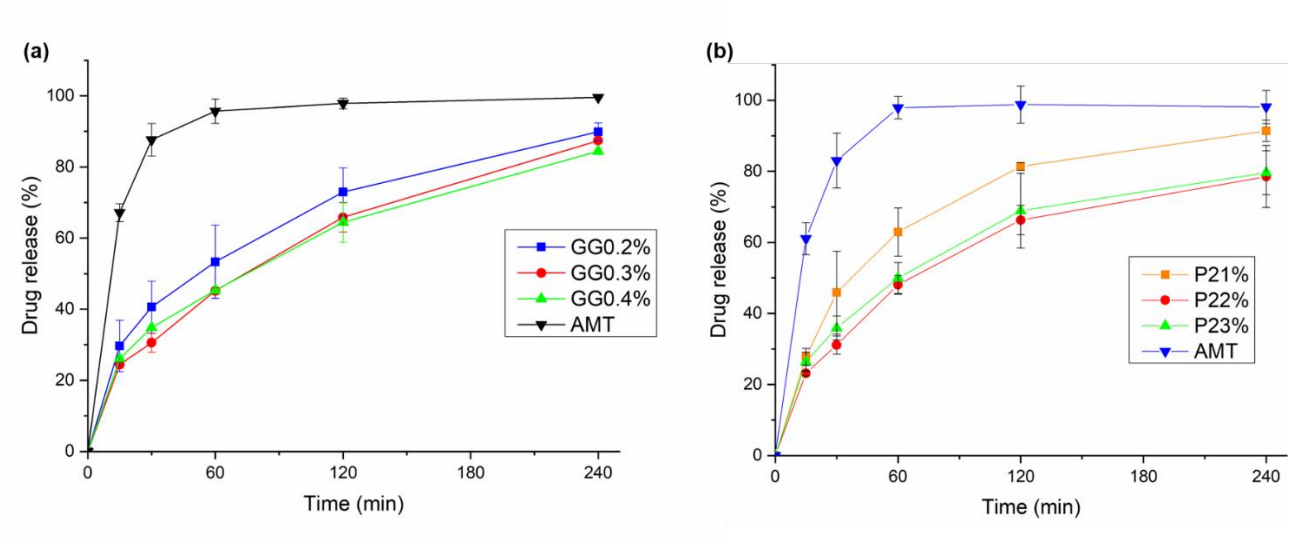

Figure 14. Drug release profile of *in situ* ionic-sensitive nasal gel of AMT (GG0.2%, GG0.3% and GG0.4%) (a) and *in situ* thermosensitive nasal gel of AMT (P21%, P22% and P23%) (b) in comparison to AMT control. Data are shown as means ± SD, n = 3.

5.7. Investigation of in vitro antibacterial activity

Antibacterial activity studies were conducted to assess the potential of *in situ* gelling AMT formulation as the alternative choice for antibiotic preparation delivered through the nasal route for the treatment of acute bacterial rhinosinusitis locally in the nasal cavity. Five common nasal pathogens (*H. influenzae*, *S. aureus*, *M. catarrhalis*, *S. pneumoniae* and *S. pyogenes*) were employed to evaluate the effectiveness of the *in situ* gelling AMT formulations [4,11], and the procedure was in accordance with the EUCAST disk diffusion method [61,109]. In this study , AMT aqueous solution was used as a positive control (PC), *in situ* gel base without AMT (22% of P407 and 0.3% GG) as negative control (NC), and all *in situ* gelling AMT formulations (P21%, P22%, P23%, GG0.2%, GG0.3% and GG0.4%) as shown in Figure 15 and 16.

After 24 h incubation time, the observations of antibacterial properties were performed. The antibacterial activity of the formulations significantly correlates with the obtained inhibitory zones [109]. The results exhibited the highest inhibitory zone was found in *M. catarrhalis* and *S. pneumoniae* cultures or both the PC (AMT solution) and all *in situ* gelling AMT formulation [110,111]. Similarly, the *in situ* gelling AMT formulation showed identical results with the PC for the diameter of inhibitory zones of *S. pyogenes*. On the other hand, a smaller inhibitory zone diameter was found in the case of *H. influenza* and *S. aureus* for the PC as well as the *in situ* gelling AMT formulations. Nevertheless, the results obtained for the *in situ* gelling AMT formulations remained nearly the same as the results shown by the PC sample. In addition, the *in situ* gel base formulation without AMT showed no antibacterial activity during the investigation.

These findings showed that there were no statistically significant differences between positive control (AMT solution) and the *in situ* gelling AMT formulation ($p > 0.05$). Accordingly, these results demonstrated that integrating the AMT-loaded BSA-NPs to the *in situ* gelling polymer (P407 and GG matrix) could successfully maintain its antibacterial capability against the five nasal pathogens in ABR. Therefore, the application of albumin-based nanoparticles incorporating into the *in situ* gelling polymer appear as a novel platform for delivering antibiotic with the purpose of local treatment in the nasal cavity as it was able to preserve the antibacterial activity of AMT and generate a prolonged drug release profile [75,112,113].

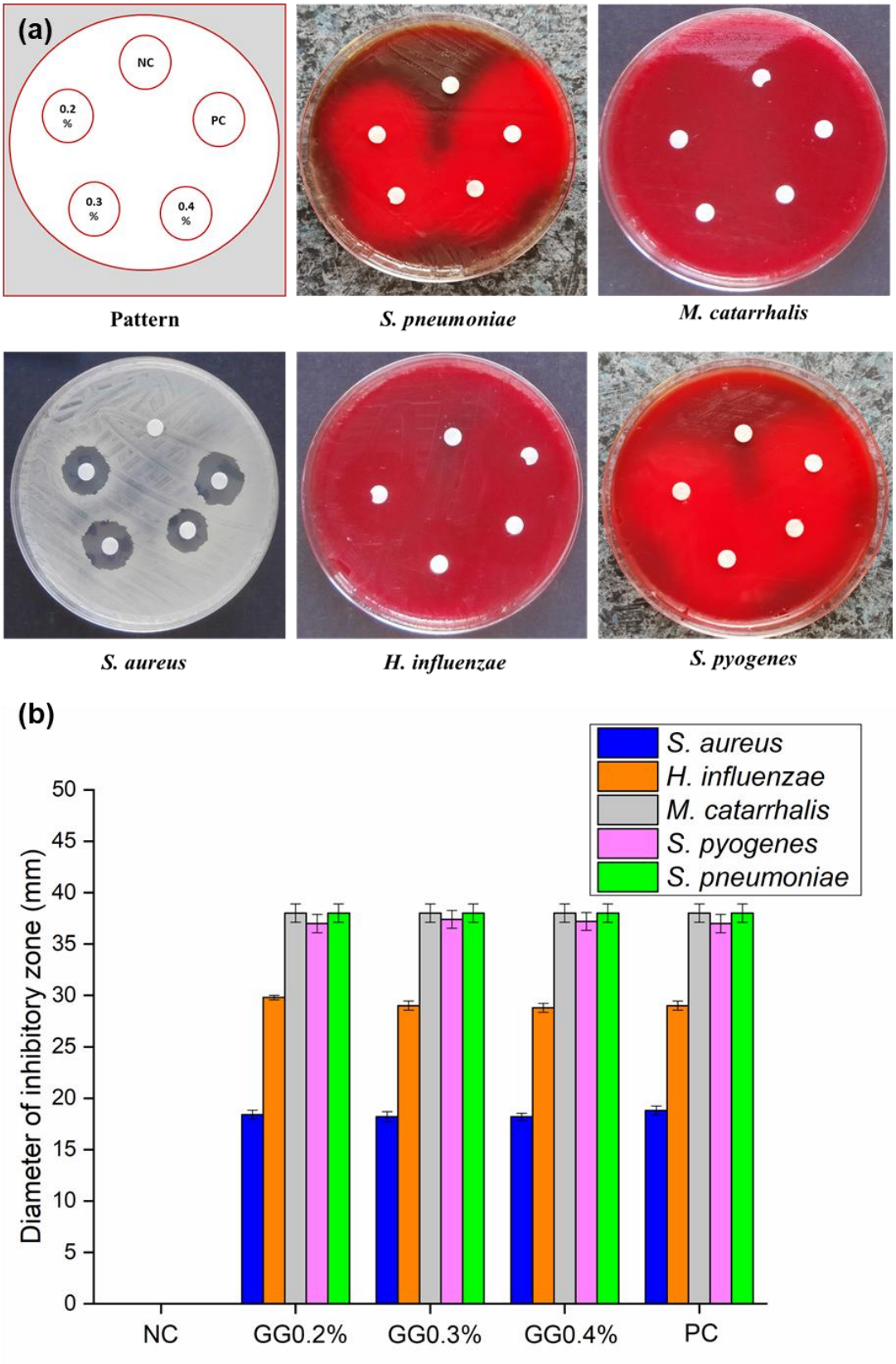

Figure 15. Disk diffusion test zone of NC, PC and *in situ* ionic-sensitive nasal gel of AMT formulations (GG0.2%, GG0.3% and GG0.4%) against five common nasal pathogens of ABR (*S. aureus*; *H. influenzae*; *M. catarrhalis*; *S. pyogenes* and *S. pneumoniae*) (A). Diameter of the inhibitory zones formed against the pathogens (B). Data are shown as means ± SD, $n = 5$.

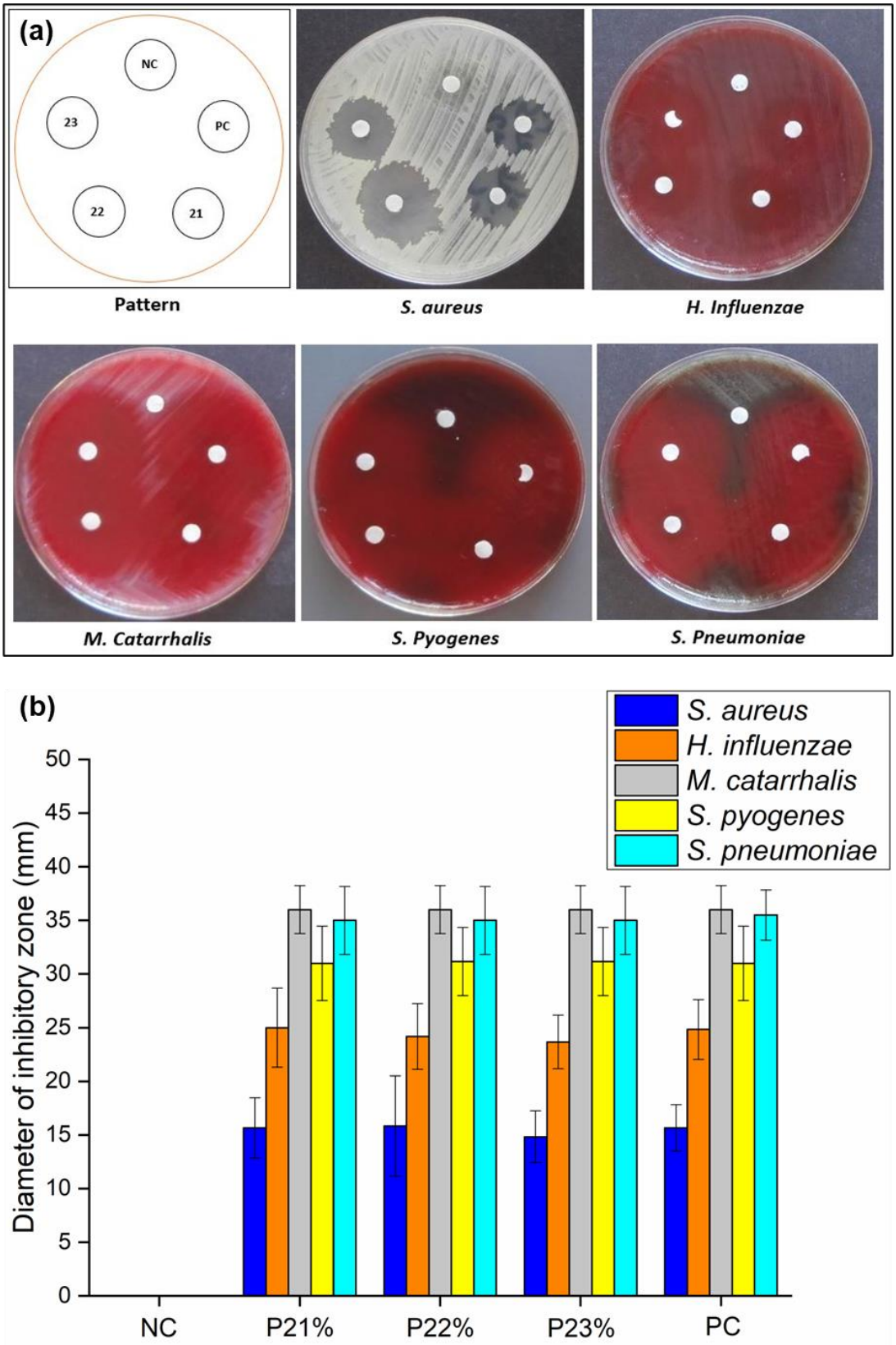

Figure 16. Disk diffusion test zone of NC, PC and *in situ* thermo-responsive nasal gel of AMT formulations (P21%, P22%, and P23%) against five common nasal pathogens of ABR (*S. aureus*; *H. influenzae*; *M. catarrhalis*; *S. pyogenes* and *S. pneumoniae*) (A). Diameter of the inhibitory zones formed against the pathogens (B). Data are shown as means ± SD, $n = 5$.

5.8. Ex vivo mucosal permeation studies

According to the results of all previous investigation, the properties of *in situ* ionic-sensitive nasal gel of AMT formulation (GG0.2%, GG0.3%, and GG0.4%) appears more suitable for nasal application with respect to its smaller particle size, proper expansion coefficient and water holding capacity, as well as the mucoadhesive behaviour, compared to the *in situ* thermo-responsive nasal gel of AMT formulation (P21%, P22%, and P23%). Therefore, the *in situ* ionic-sensitive nasal gel of AMT was employed for further investigation step; the *ex-vivo* mucosal permeation studies [114].

The e*x vivo* mucosal permeation study of the *in situ* ionic-sensitive nasal gel of AMT formulations and aqueous AMT solution (1 mg/ml) were executed using a modified Side-Bi-Side® type permeation cell using human nasal mucosa. The Side-Bi-Side® type horizontal diffusion cell is widely recommended for the investigation of nasal liquid preparations [115] as in present case for the *in situ* ionic-sensitive nasal gel of AMT formulations. In this circumstance, the cumulative permeation of AMT through the human nasal mucosa and the apparent permeability coefficient (P_{app}) are suitable parameters to characterize the nasal penetration of drug. Both mentioned parameters were determined after 60 min treatment. As graphically illustrated in Figure 17A, the mass permeated after 60 min in the case of AMT solution was significantly higher ($p<0.05$) compared to that of *in situ* gelling AMT formulations. The permeation profile of the *in situ* gelling formulations of AMT could be attributed to gelling properties of GG which immediately undergo sol to gel once in contact with SNES medium in the acceptor compartment, then able to retain the drug without permeating through the membrane.

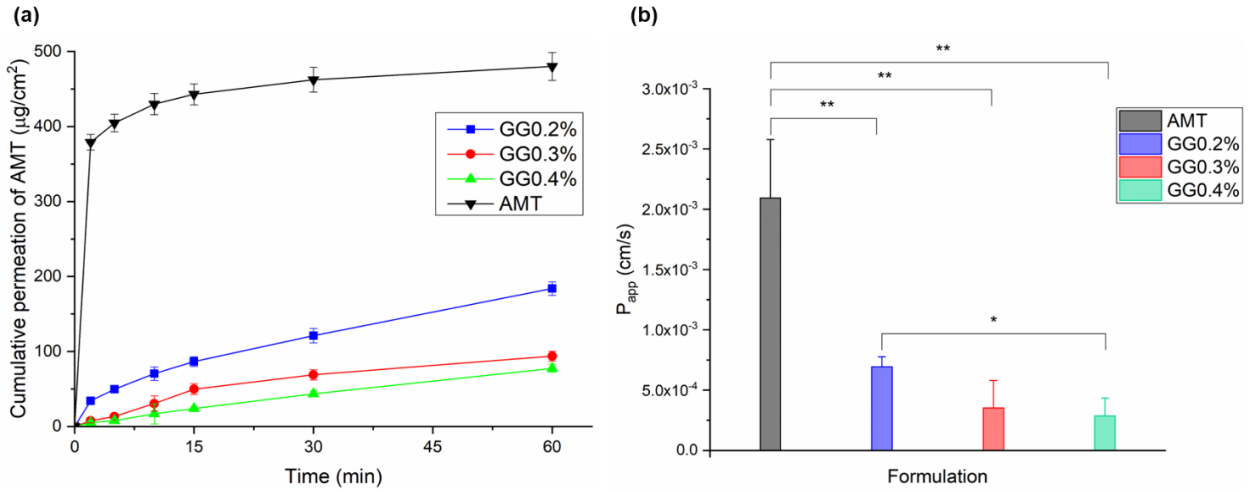

Figure 17. Cumulative permeation curves (a) and apparent permeability (b) of the *in situ* gelling AMT formulations: GG0.2%, GG0.3%, and GG0.4%; compared to the AMT solution (1 mg/ml) as control during 60 minutes of treatment. Data are shown as means ± SD, $n = 3$. Significant differences are indicated with asterisks (*$p<0.05$ and **$p<0.01$).

Moreover, the role of BSA nanoparticles which have sustained release properties [116] and attributed to their low permeability was also considerable in protecting the release of AMT against nasal conditions [111]. Figure 17B shows the P_{app} value of the AMT solution was also significantly higher ($p<0.05$) compared to the *in situ* gelling AMT formulations, moreover the GG0.4% indicates significantly lower ($p<0.05$) P_{app} value in comparison to GG0.2%. All these parameters were inversely proportional to the GG concentration, an increased gel strength by increasing the GG concentration in the formulations resulted in higher retention of AMT in the gel matrix, supporting the application for local therapeutic effect and hindered systemic absorption [101].

5.9. Ex vivo recovery and extraction assays

The aim of this work was to develop *in situ* ionic sensitive gel of AMT for local therapy in nasal cavity. In this circumstances, the AMT was intended to be retained in the nasal mucosa instead of permeating through the membrane. Therefore, it is important to investigate the amount of AMT retained in the nasal mucosa, in order to evaluate the ability of the formulation to hold the drug in the gel matrix, which further greatly influence the efficacy of the treatment. The results showed that GG0.4% showed the lowest amount of AMT, approximately 0.180 µg/mg. This demonstrated that the drug was entrapped in the gel matrix of GG0.4% formulation and because of its high viscosity, then the AMT was not able to permeate to the nasal mucosa. Moreover, higher amount of AMT was found on the nasal mucosa for GG0.3% and GG0.2%, which were around 0.298 µg/mg and 0.378 µg/mg, respectively, compared the AMT solution as control with 3.314 µg/mg amount of retained AMT. These findings were also in line with previous results of *ex vivo* permeation studies, as presented by the low amount of drug permeated and inversely proportional to the GG concentration used in the formulation. Hence, this investigation indicated the potential of the *in situ* ionic sensitive gel of AMT formulation to retain the drug locally in the nasal tissue.

5.10. Ex vivo retention test by Raman Chemical Mapping

Raman chemical mapping was utilized to investigate the retention properties of the *in situ* gelling AMT formulation in order to ensure its applicability is suitable for the treatment intended for localized effect on the nasal mucosa in comparison to the AMT solution. For localization of AMT within the cross-sectional slice of nasal mucosa, the Raman spectrum of pure AMT was utilized as a reference. The frequency of occurrence was visually represented in the chemical maps, correlating to the statistical distribution of specific chemical constituents (Figure 18). Various colors of the chemical map demonstrate the relative intensity change of AMT in each region of the tissue. The red area indicates the availability of AMT in high intensity, while the green area denotes zones that are related to the formulation's components, including water, BSA, and gellan gum; and then

the blue part depicts regions with distinct spectral resolution, which are the characteristics of the nasal mucosa tissue [62]. The results revealed that in the case of *in situ* gelling AMT formulation, the mucosal distribution correlation maps demonstrated a remarkable Raman intensity in the upper part of nasal mucosa specimens, corresponding to the high content of protein of the nasal epithelial layer. Meanwhile, for AMT solution, strong existence of AMT was detected in the whole cross-section of the nasal mucosa indicating remarkable penetration of drug and presuming high systemic absorption. Notably, the findings were reliable with the results of *ex vivo* permeation studies. Therefore, this investigation indicated that the *in situ* gelling AMT formulations is instead in the mucosa surface than permeating across the nasal mucosa membrane; therefore, it could be suitable for treating a local infection in the nasal cavity.

Based on the findings presented here, it is clear that the formulation of mucoadhesive *in situ* nasal gel of amoxicillin trihydrate was able to provide great potential for local treatment in nasal mucosa. The formulation of GG0.3% showed proper characteristics based on the mucoadhesive properties and the ability to retain the drug. From these findings, some extensive investigations are essential to take into consideration for future actions to completely explore the efficacy and effectiveness of this preparation as well as to guarantee the usability of this delivery systems.

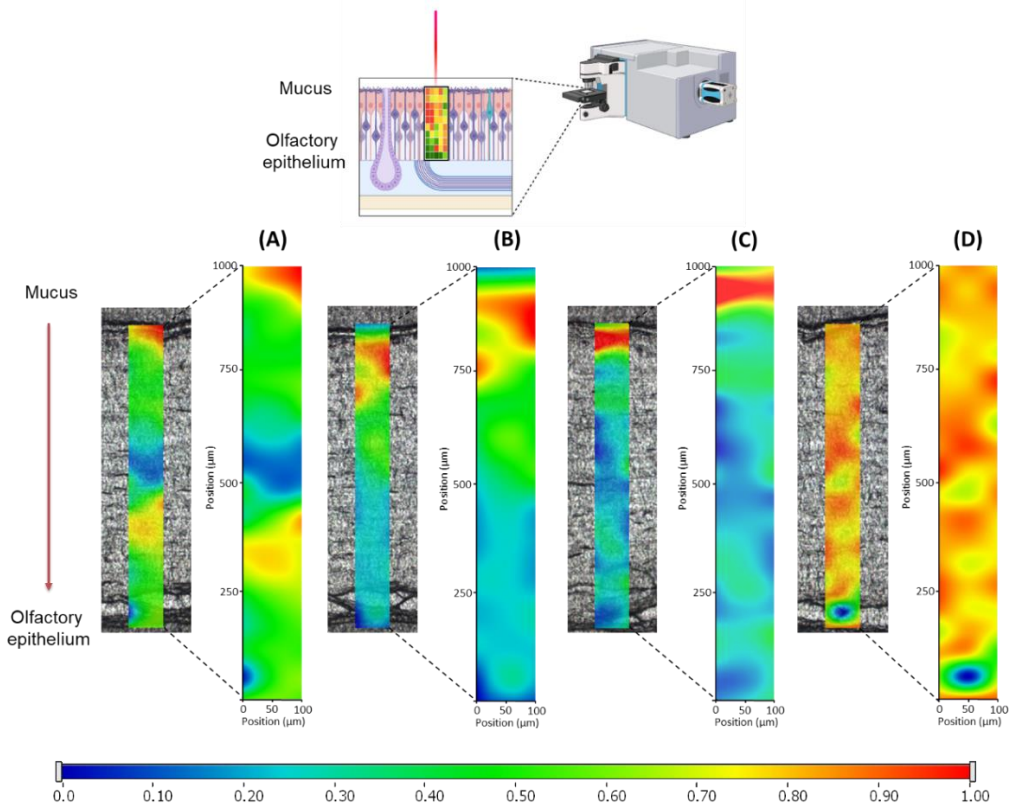

Figure 18. Raman correlation mapping of the *in situ* gelling AMT formulations: (A) GG0.2%, (B) GG0.3%, and (C) GG0.4%, in comparison to (D) AMT solution (1 mg/ml).

6. CONCLUSION

Amoxicillin-loaded albumin nanoparticles incorporated into *in situ* gelling polymer matrices (P407 or GG) may become a valuable alternative to oral antibiotic therapy with the aim for an effective treatment of local nasal bacterial infections, such as ABR. The application of an *in situ* gelling system embedded albumin-based nanocarrier with the aim of local nasal antibiotic therapy was a novel approach utilizing the slow diffusion of BSA nanoparticles in polymer matrix, therefore reducing mucosal absorption and increase residence time which further supported the prolonged drug release in the nasal cavity. The main conclusions can be summarized in the following points:

1. The optimization of albumin-based nanoparticles utilizing a 3-factor, 3-level of full factorial design successfully generated the appropriate composition of BSA, ethanol, and purified water for fabricating albumin-based nanoparticles in nanosized range suitable for nasal administration.

2. The obtained amoxicillin-loaded BSA incorporated into *in situ* gelling system showed higher entrapment efficiency with proper essential parameters for nasal administration, such as expansion coefficient, water holding capacity, and rheological properties. In this work, the concentration of 21% P407 and 0.3% gellan gum can be considered as suitable concentrations for preparing *in situ* nasal gel of AMT for enhanced nasal applicability.

3. The utilization of *in situ* gelling system could be a promising approach to effectively administer AMT via nasal delivery route. In this work, noteworthy outcomes were attained concerning crucial characteristics of nasal formulation, which in this case, the *in situ* ionic-sensitive polymer matrices exhibited adequate mucoadhesive properties with appropriate *in vitro* drug release profile, facilitating the AMT formulation to stay longer in the nasal cavity.

4. *In vitro* antibacterial activity studies revealed that the effectiveness of AMT against five common nasal pathogens in ABR remained stable and can maintain its efficacy in the form of *in situ* gelling nasal gel formulations. Therefore, the incorporation of amoxicillin-loaded BSA nanoparticles into *in situ* gelling polymers appears to be a promising approach to overcome the limitation of nasal route administration and to effectively deliver antibiotic therapy for local nasal bacterial infection.

5. The *ex vivo* permeability and retention studies revealed that the *in situ* ionic-sensitive nasal gel of AMT formulations were able to retain the drug on the surface of the human nasal mucosa tissue instead of directly penetrating through the membrane, confirming its potential for

treating nasal infections locally. This work demonstrates that the *in situ* gelling systems exhibited potential as a delivery vehicle for improved nasal applicability of AMT for local therapeutic purpose.

7. NOVELTY AND PRACTICAL ASPECTS

The main new findings and practical aspects of the work can be summarized by the following:

1. The Ph.D. thesis aimed to develop nasal drug administration of antibiotic substances for local nasal therapeutic purpose. To date, the orally administered antibiotics have been the only treatment option for ABR so far. Therefore, this research showed the possibility of delivering antibiotic substance to treat nasal infections directly to the infection site, minimizing the adverse effect, and establishing proper use of antibiotic.

2. The important step for developing nasal antibiotic formulation can be achieved through determining the therapeutic target, then considering the challenges and limitation in nasal route delivery. Following this, appropriate formulation strategy and approach can be established to achieve successful fabricating of nasal antibiotic formulation.

3. A novel strategy of developing nasal antibiotic formulation has been demonstrated, and this method opens up more way of nasal drug formulation possibilities in a liquid dosage forms containing active substances which is not very soluble in water, taking into account the requirements for both the nasal delivery method and the nanoparticulate systems.

4. The integration of albumin-based nanoparticles into the *in situ* gelling polymers presents a valuable and promising nasal drug delivery approach. This combination exhibits significant potential to overcome nasal route challenges, facilitating adequate mucoadhesion, and allowing remarkable drug release properties, while preserving the efficacy of antibiotic substance.

5. The successful retention behavior of AMT in the form of *in situ* ionic-sensitive nasal gel formulation on the surface of human nasal mucosa tissue, instead of directly penetrating through the mucosa membrane, proves that nasal formulation utilizing *in-situ* gelling systems as delivery vehicle have the great potential to be an effective way for delivering antibiotic substances via the nasal route administration for local therapeutic purposes.

8. REFERENCES

1. Rovelsky, S.A.; Remington, R.E.; Nevers, M.; Pontefract, B.; Hersh, A.L.; Samore, M.; Madaras-Kelly, K. Comparative Effectiveness of Amoxicillin versus Amoxicillin-clavulanate among Adults with Acute Sinusitis in Emergency Department and Urgent Care Settings. *J. Am. Coll. Emerg. Physicians Open* **2021**, *2*, 1–8, doi:10.1002/emp2.12465.
2. Rosenfeld, R.M.; Piccirillo, J.F.; Chandrasekhar, S.S.; Brook, I.; Ashok Kumar, K.; Kramper, M.; Orlandi, R.R.; Palmer, J.N.; Patel, Z.M.; Peters, A.; et al. Clinical Practice Guideline (Update): Adult Sinusitis. *Otolaryngol. - Head Neck Surg. (United States)* **2015**, *152*, S1–S39, doi:10.1177/0194599815572097.
3. Axiotakis, L.G.; Szeto, B.; Gonzalez, J.N.; Caruana, F.F.; Gudis, D.A.; Overdevest, J.B. Antibiotic Adverse Effects in Pediatric Acute Rhinosinusitis: Systematic Review and Meta-Analysis. *Int. J. Pediatr. Otorhinolaryngol.* **2022**, *156*, 1–10, doi:10.1016/j.ijporl.2022.111064.
4. Lemiengre, M..; van Driel, M..; Merestein, D.; Liira, H.; Makela, M.; De Sutter, A.I.. Antibiotics for Acute Rhinosinusitis in Adults (Review). *Cochrane Database Syst. Rev.* **2018**, *2018*, 1–80, doi:10.1002/14651858.CD006089.pub5.
5. Homayun, B.; Lin, X.; Choi, H. Challenges and Recent Progress in Oral Drug Delivery Systems for Biopharmaceuticals. *Pharmaceutics* **2019**, *11*, 1–29, doi:10.3390/pharmaceutics11030129.
6. Velde, F. De; Winter, B.C.M. De; Koch, B.C.P.; Gelder, T. Van; Mouton, J.W. Non-Linear Absorption Pharmacokinetics of Amoxicillin : Consequences for Dosing Regimens and Clinical Breakpoints. *J. Antimicrob. Chemother.* **2016**, *71*, 2909–2917, doi:10.1093/jac/dkw226.
7. Huttner, A.; Bielicki, J.; Clements, M.N.; Frimodt-Møller, N.; Muller, A.E.; Paccaud, J.P.; Mouton, J.W. Oral Amoxicillin and Amoxicillin–Clavulanic Acid: Properties, Indications and Usage. *Clin. Microbiol. Infect.* **2020**, *26*, 871–879, doi:10.1016/j.cmi.2019.11.028.
8. Keller, L.A.; Merkel, O.; Popp, A. Intranasal Drug Delivery: Opportunities and Toxicologic Challenges during Drug Development. *Drug Deliv. Transl. Res.* **2021**, 1–23, doi:10.1007/s13346-020-00891-5.
9. Cingi, C.; Bayar Muluk, N.; Mitsias, D.I.; Papadopoulos, N.G.; Klimek, L.; Laulajainen-Hongisto, A.; Hytönen, M.; Toppila-Salmi, S.K.; Scadding, G.K. The Nose as a Route for Therapy: Part 1. Pharmacotherapy. *Front. Allergy* **2021**, *2*, 1–17, doi:10.3389/falgy.2021.638136.
10. van de Beek, D.; Cabellos, C.; Dzupova, O.; Esposito, S.; Klein, M.; Kloek, A.T.; Leib, S.L.; Mourvillier, B.; Ostergaard, C.; Pagliano, P.; et al. ESCMID Guideline: Diagnosis and Treatment of Acute Bacterial Meningitis. *Clin. Microbiol. Infect.* **2016**, *22*, S37–S62, doi:10.1016/j.cmi.2016.01.007.
11. Patel, Z.M.; Hwang, P.H. Acute Bacterial Rhinosinusitis. In *Infections of the Ears, Nose, Throat, and Sinuses*; Durand, M.., Deschler, D.., Eds.; Springer International Publishing AG, part of Springer Nature: New York City, United States, 2018; pp. 1–143 ISBN 9783319748351.
12. Brook, I. Microbiology of Chronic Rhinosinusitis. *Eur. J. Clin. Microbiol. Infect. Dis.* **2016**, *35*, 1059–1068, doi:10.1007/s10096-016-2640-x.
13. Rawlings, B.A.; Higgins, T.S.; Han, J.K. Bacterial Pathogens in the Nasopharynx, Nasal Cavity, and Osteomeatal Complex during Wellness and Viral Infection. *Am. J. Rhinol. Allergy* **2013**, *27*, 39–42, doi:10.2500/ajra.2013.27.3835.
14. Mardikasari, S.A.; Sipos, B.; Csóka, I.; Katona, G. Nasal Route for Antibiotics Delivery: Advances, Challenges and Future Opportunities Applying the Quality by Design Concepts. *J. Drug Deliv. Sci. Technol.* **2022**, *77*, 1–18, doi:10.1016/j.jddst.2022.103887.
15. Kublik, H.; Vidgren, M.. Nasal Delivery Systems and Their Effect on Deposition and Absorption. *Adv. Drug Deliv. Rev.* **1998**, *29*, 157–177, doi:10.3109/9781420086713-10.
16. Schriever, V.A.; Hummel, T.; Lundström, J.N.; Freiherr, J. Size of Nostril Opening as a Measure of Intranasal Volume. *Physiol. Behav.* **2013**, *110–111*, 3–5,

doi:10.1016/j.physbeh.2012.12.007.
17. Kahana-Zweig, R.; Geva-Sagiv, M.; Weissbrod, A.; Secundo, L.; Soroker, N.; Sobel, N. Measuring and Characterizing the Human Nasal Cycle. *PLoS One* **2016**, *11*, 1–28, doi:10.1371/journal.pone.0162918.
18. Marks, T.N.; Maddux, S.D.; Butaric, L.N.; Franciscus, R.G. Climatic Adaptation in Human Inferior Nasal Turbinate Morphology: Evidence from Arctic and Equatorial Populations. *Am. J. Phys. Anthropol.* **2019**, *169*, 498–512, doi:10.1002/ajpa.23840.
19. Ugwoke, M.I.; Verbeke, N.; Kinget, R. The Biopharmaceutical Aspects of Nasal Mucoadhesive Drug Delivery. *J. Pharm. Pharmacol.* **2001**, *53*, 3–21, doi:10.1211/0022357011775145.
20. Gizurarson, S. Anatomical and Histological Factors Affecting Intranasal Drug and Vaccine Delivery. *Curr. Drug Deliv.* **2012**, *9*, 566–582, doi:10.2174/156720112803529828.
21. Mygind, N.; Dahl, R. Anatomy, Physiology and Function of the Nasal Cavities in Health and Disease. *Adv. Drug Deliv. Rev.* **1998**, *29*, 3–12, doi:10.1016/S0169-409X(97)00058-6.
22. Longest, P.W.; Golshahi, L.; Behara, S.R.B.; Tian, G.; Farkas, D.R.; Hindle, M. Efficient Nose-to-Lung (N2L) Aerosol Delivery with a Dry Powder Inhaler. *J. Aerosol Med. Pulm. Drug Deliv.* **2015**, *28*, 189–201, doi:10.1089/jamp.2014.1158.
23. Klodzińska, S.N.; Priemel, P.A.; Rades, T.; Nielsen, H.M. Inhalable Antimicrobials for Treatment of Bacterial Biofilm-Associated Sinusitis in Cystic Fibrosis Patients: Challenges and Drug Delivery Approaches. *Int. J. Mol. Sci.* **2016**, *17*, 1–20, doi:10.3390/ijms17101688.
24. Xi, J.; Lei, L.R.; Zouzas, W.; April Si, X. Nasally Inhaled Therapeutics and Vaccination for COVID-19: Developments and Challenges. *MedComm* **2021**, *2*, 569–586, doi:10.1002/mco2.101.
25. Jones, N. The Nose and Paranasal Sinuses Physiology and Anatomy. *Adv. Drug Deliv. Rev.* **2001**, *51*, 5–19, doi:10.1016/S0169-409X(01)00172-7.
26. Quraishi, M.S.; Jones, N.S.; Mason, J. The Rheology of Nasal Mucus: A Review. *Clin. Otolaryngol. Allied Sci.* **1998**, *23*, 403–413, doi:10.1046/j.1365-2273.1998.00172.x.
27. Emad, N.A.; Ahmed, B.; Alhalmi, A.; Alzobaidi, N.; Al-Kubati, S.S. Recent Progress in Nanocarriers for Direct Nose to Brain Drug Delivery. *J. Drug Deliv. Sci. Technol.* **2021**, *64*, 1–11, doi:10.1016/j.jddst.2021.102642.
28. Zahir-Jouzdani, F.; Wolf, J.D.; Atyabi, F.; Bernkop-Schnürch, A. In Situ Gelling and Mucoadhesive Polymers: Why Do They Need Each Other? *Expert Opin. Drug Deliv.* **2018**, *15*, 1007–1019, doi:10.1080/17425247.2018.1517741.
29. Agrawal, M.; Saraf, S.; Saraf, S.; Dubey, S.K.; Puri, A.; Gupta, U.; Kesharwani, P.; Ravichandiran, V.; Kumar, P.; Naidu, V.G.M.; et al. Stimuli-Responsive In Situ Gelling System for Nose-to-Brain Drug Delivery. *J. Control. Release* **2020**, *327*, 235–265, doi:10.1016/j.jconrel.2020.07.044.
30. Chen, Y.; Lee, J.; Meng, M.; Cui, N.; Dai, C.Y.; Jia, Q.; Lee, E.; Chen, Y.; Chen, Y.; Lee, J.; et al. An Overview on Thermosensitive Oral Gel Based on An Overview on Thermosensitive Oral Gel Based on Poloxamer. *Materials (Basel).* **2021**, *14*, 1–20, doi:10.3390/ma14164522.
31. Matanović, M.R.; Kristl, J.; Grabnar, P.A. Thermoresponsive Polymers: Insights into Decisive Hydrogel Characteristics, Mechanisms of Gelation, and Promising Biomedical Applications. *Int. J. Pharm.* **2014**, *472*, 262–275, doi:10.1016/j.ijpharm.2014.06.029.
32. Giuliano, E.; Paolino, D.; Fresta, M.; Cosco, D. Mucosal Applications of Poloxamer 407-Based Hydrogels: An Overview. *Pharmaceutics* **2018**, *10*, 1–26, doi:10.3390/pharmaceutics10030159.
33. Katona, G.; Sipos, B.; Budai-Szűcs, M.; Balogh, G.T.; Veszelka, S.; Gróf, I.; Deli, M.A.; Volk, B.; Szabó-Révész, P.; Csóka, I. Development of in Situ Gelling Meloxicam-Human Serum Albumin Nanoparticle Formulation for Nose-to-Brain Application. *Pharmaceutics* **2021**, *13*, 1–22, doi:10.3390/pharmaceutics13050646.
34. Jelkmann, M.; Leichner, C.; Zaichik, S.; Laffleur, F.; Bernkop-Schnürch, A. A Gellan Gum

Derivative as In-Situ Gelling Cationic Polymer for Nasal Drug Delivery. *Int. J. Biol. Macromol.* **2020**, *158*, 1037–1046, doi:10.1016/j.ijbiomac.2020.04.114.
35. Friedman, N.D.; Temkin, E.; Carmeli, Y. The Negative Impact of Antibiotic Resistance. *Clin. Microbiol. Infect.* **2016**, *22*, 416–422, doi:10.1016/j.cmi.2015.12.002.
36. Lux, C.A.; Wagner Mackenzie, B.; Johnston, J.; Zoing, M.; Biswas, K.; Taylor, M.W.; Douglas, R.G. Antibiotic Treatment for Chronic Rhinosinusitis: Prescription Patterns and Associations With Patient Outcome and the Sinus Microbiota. *Front. Microbiol.* **2020**, *11*, 1–11, doi:10.3389/fmicb.2020.595555.
37. Mardikasari, S.A.; Katona, G.; Sipos, B.; Csóka, I. Expert Opinion on Drug Delivery Essential Considerations Towards Development of Effective Nasal Antibiotic Formulation : Features, Strategies, and Future Directions. *Expert Opin. Drug Deliv.* **2024**, 1–15, doi:10.1080/17425247.2024.2341184.
38. Arabi, S.H.; Haselberger, D.; Hinderberger, D. The Effect of Ethanol on Gelation, Nanoscopic, and Macroscopic Properties of Serum Albumin Hydrogels. *Molecules* **2020**, *25*, doi:10.3390/molecules25081927.
39. Sanaeifar, N.; Mäder, K.; Hinderberger, D. Nanoscopic Characterization of Stearic Acid Release from Bovine Serum Albumin Hydrogels. *Macromol. Biosci.* **2020**, *20*, doi:10.1002/mabi.202000126.
40. Jahanban-Esfahlan, A.; Dastmalchi, S.; Davaran, S. A Simple Improved Desolvation Method for the Rapid Preparation of Albumin Nanoparticles. *Int. J. Biol. Macromol.* **2016**, *91*, 703–709, doi:10.1016/j.ijbiomac.2016.05.032.
41. Langer, K.; Balthasar, S.; Vogel, V.; Dinauer, N.; Von Briesen, H.; Schubert, D. Optimization of the Preparation Process for Human Serum Albumin (HSA) Nanoparticles. *Int. J. Pharm.* **2003**, *257*, 169–180, doi:10.1016/S0378-5173(03)00134-0.
42. Amighi, F.; Emam-Djomeh, Z.; Labbafi-Mazraeh-Shahi, M. Effect of Different Cross-Linking Agents on the Preparation of Bovine Serum Albumin Nanoparticles. *J. Iran. Chem. Soc.* **2020**, *17*, 1223–1235, doi:10.1007/s13738-019-01850-9.
43. Karami, K.; Jamshidian, N.; Hajiaghasi, A.; Amirghofran, Z. BSA Nanoparticles as Controlled Release Carriers for Isophethalaldoxime Palladacycle Complex; Synthesis, Characterization,: In Vitro Evaluation, Cytotoxicity and Release Kinetics Analysis. *New J. Chem.* **2020**, *44*, 4394–4405, doi:10.1039/c9nj05847h.
44. Youssef, N.A.H.A.; Kassem, A.A.; Farid, R.M.; Ismail, F.A.; EL-Massik, M.A.E.; Boraie, N.A. A Novel Nasal Almotriptan Loaded Solid Lipid Nanoparticles in Mucoadhesive in Situ Gel Formulation for Brain Targeting: Preparation, Characterization and in Vivo Evaluation. *Int. J. Pharm.* **2018**, *548*, 609–624, doi:10.1016/j.ijpharm.2018.07.014.
45. Huang, G.; Xie, J.; Shuai, S.; Wei, S.; Chen, Y.; Guan, Z.; Zheng, Q.; Yue, P.; Wang, C. Nose-to-Brain Delivery of Drug Nanocrystals by Using Ca2+ Responsive Deacetylated Gellan Gum Based in Situ-Nanogel. *Int. J. Pharm.* **2021**, *594*, 120182, doi:10.1016/j.ijpharm.2020.120182.
46. Hao, J.; Zhao, J.; Zhang, S.; Tong, T.; Zhuang, Q.; Jin, K.; Chen, W.; Tang, H. Fabrication of an Ionic-Sensitive in Situ Gel Loaded with Resveratrol Nanosuspensions Intended for Direct Nose-to-Brain Delivery. *Colloids Surfaces B Biointerfaces* **2016**, *147*, 376–386, doi:10.1016/j.colsurfb.2016.08.011.
47. Hosny, K.M.; Hassan, A.H. Intranasal in Situ Gel Loaded with Saquinavir Mesylate Nanosized Microemulsion: Preparation, Characterization, and in Vivo Evaluation. *Int. J. Pharm.* **2014**, *475*, 191–197, doi:10.1016/j.ijpharm.2014.08.064.
48. Chen, Y.; Liu, Y.; Xie, J.; Zheng, Q.; Yue, P.; Chen, L.; Hu, P.; Yang, M. Nose-to-Brain Delivery by Nanosuspensions-Based in Situ Gel for Breviscapine. *Int. J. Nanomedicine* **2020**, *15*, 10435–10451, doi:10.2147/IJN.S265659.
49. Salunke, S.R.; Patil, S.B. Ion Activated in Situ Gel of Gellan Gum Containing Salbutamol Sulphate for Nasal Administration. *Int. J. Biol. Macromol.* **2016**, *87*, 41–47, doi:10.1016/j.ijbiomac.2016.02.044.

50. Mao, R.; Tang, J.; Swanson, B.G. Water Holding Capacity and Microstructure of Gellan Gels. *Carbohydr. Polym.* **2001**, *46*, 365–371, doi:10.1016/S0144-8617(00)00337-4.
51. Lungare, S.; Bowen, J.; Badhan, R. Development and Evaluation of a Novel Intranasal Spray for the Delivery of Amantadine. *J. Pharm. Sci.* **2016**, *105*, 1209–1220, doi:10.1016/j.xphs.2015.12.016.
52. Trenkel, M.; Scherließ, R. Nasal Powder Formulations: In-Vitro Characterisation of the Impact of Powders on Nasal Residence Time and Sensory Effects. *Pharmaceutics* **2021**, *13*, doi:10.3390/pharmaceutics13030385.
53. Yu, Y.S.; AboulFotouh, K.; Xu, H.; Williams, G.; Suman, J.; Cano, C.; Warnken, Z.N.; Wu, K.C.W.; Williams, R.O.; Cui, Z. Feasibility of Intranasal Delivery of Thin-Film Freeze-Dried, Mucoadhesive Vaccine Powders. *Int. J. Pharm.* **2023**, *640*, 122990, doi:10.1016/j.ijpharm.2023.122990.
54. Chen, X.; Yan, J.; Yu, S.; Wang, P. Formulation and In Vitro Release Kinetics of Mucoadhesive Blend Gels Containing Matrine for Buccal Administration. *AAPS J.* **2018**, *19*, 470–480, doi:10.1208/s12249-017-0853-7.
55. Cook, S.L.; Bull, S.P.; Methven, L.; Parker, J.K.; Khutoryanskiy, V. V Food Hydrocolloids Mucoadhesion : A Food Perspective. *Food Hydrocoll.* **2017**, *72*, 281–296, doi:10.1016/j.foodhyd.2017.05.043.
56. Khutoryanskiy, V. V Advances in Mucoadhesion and Mucoadhesive Polymers. *Macromol. Biosci.* **2011**, *11*, 748–764, doi:10.1002/mabi.201000388.
57. Syed, M.A.; Hanif, S.; Ain, N.; Syed, H.K.; Zahoor, A.F.; Khan, I.U.; Abualsunun, W.A.; Jali, A.M.; Qahl, S.H.; Sultan, M.H.; et al. Assessment of Binary Agarose – Carbopol Buccal Gels for Mucoadhesive Drug Delivery : Ex Vivo and In Vivo Characterization. *Molecules* **2022**, *27*, 1–20, doi:10.3390/molecules27207004.
58. Illum, L. Nasal Clearance in Health and Disease. *J. Aerosol Med.* **2006**, *19*, 92–99.
59. Inoue, D.; Tanaka, A.; Kimura, S.; Kiriyama, A.; Katsumi, H.; Yamamoto, A.; Ogawara, K. ichi; Kimura, T.; Higaki, K.; Yutani, R.; et al. The Relationship between in Vivo Nasal Drug Clearance and in Vitro Nasal Mucociliary Clearance: Application to the Prediction of Nasal Drug Absorption. *Eur. J. Pharm. Sci.* **2018**, *117*, 21–26, doi:10.1016/j.ejps.2018.01.032.
60. Moreno-Bautista, G.; Tam, K.C. Evaluation of Dialysis Membrane Process for Quantifying the in Vitro Drug-Release from Colloidal Drug Carriers. *Colloids Surfaces A Physicochem. Eng. Asp.* **2011**, *389*, 299–303, doi:10.1016/j.colsurfa.2011.07.032.
61. The European Committee on Antimicrobial Susceptibility Testing (EUCAST) Disk Diffusion Method for Antimicrobial Susceptibility Testing Version 10.0 Available online: https://www.eucast.org/ast_of_bacteria/disk_diffusion_methodology/ (accessed on 27 August 2022).
62. Sipos, B.; Bella, Z.; Gróf, I.; Veszelka, S.; Deli, M.A.; Szűcs, K.F.; Sztojkov-Ivanov, A.; Ducza, E.; Gáspár, R.; Kecskeméti, G.; et al. Soluplus® Promotes Efficient Transport of Meloxicam to the Central Nervous System via Nasal Administration. *Int. J. Pharm.* **2023**, *632*, doi:10.1016/j.ijpharm.2023.122594.
63. Katona, G.; Sabir, F.; Sipos, B.; Naveed, M.; Schelz, Z.; Zupkó, I.; Csóka, I. Development of Lomustine and N-Propyl Gallate Co-Encapsulated Liposomes for Targeting Glioblastoma Multiforme via Intranasal Administration. *Pharmaceutics* **2022**, *14*, doi:10.3390/pharmaceutics14030631.
64. Weber, C.; Coester, C.; Kreuter, J.; Langer, K. Desolvation Process and Surface Characterisation of Protein Nanoparticles. *Int. J. Pharm.* **2000**, *194*, 91–102, doi:10.1016/S0378-5173(99)00370-1.
65. Tarhini, M.; Benlyamani, I.; Hamdani, S.; Agusti, G.; Fessi, H.; Greige-Gerges, H.; Bentaher, A.; Elaissari, A. Protein-Based Nanoparticle Preparation via Nanoprecipitation Method. *Materials (Basel).* **2018**, *11*, 1–18, doi:10.3390/ma11030394.
66. David, C.; Foley, S.; Mavon, C.; Enescu, M. Reductive Unfolding of Serum Albumins

Uncovered by Raman Spectroscopy. *Biopolymers* **2008**, *89*, 623–634, doi:10.1002/bip.20972.
67. Emin, A.; Hushur, A.; Mamtimin, T. Raman Study of Mixed Solutions of Methanol and Ethanol. *AIP Adv.* **2020**, *10*, doi:10.1063/1.5140722.
68. European Medicines Agency (EMA) *ICH Guideline Q3C (R5) on Impurities: Guideline for Residual Solvents*; 2006;
69. Tang, B.; Fang, G.; Gao, Y.; Liu, Y.; Liu, J.; Zou, M.; Cheng, G. Liprosomes Loading Paclitaxel for Brain-Targeting Delivery by Intravenous Administration: In Vitro Characterization and in Vivo Evaluation. *Int. J. Pharm.* **2014**, *475*, 416–427, doi:10.1016/j.ijpharm.2014.09.011.
70. Kang, Y.; Yang, C.; Ouyang, P.; Yin, G.; Huang, Z.; Yao, Y.; Liao, X. The Preparation of BSA-PLLA Microparticles in a Batch Supercritical Anti-Solvent Process. *Carbohydr. Polym.* **2009**, *77*, 244–249, doi:10.1016/j.carbpol.2008.12.029.
71. Spada, A.; Emami, J.; Tuszynski, J.A.; Lavasanifar, A. The Uniqueness of Albumin as a Carrier in Nanodrug Delivery. *Mol. Pharm.* **2021**, *18*, 1862–1894, doi:10.1021/acs.molpharmaceut.1c00046.
72. Hornok, V. Serum Albumin Nanoparticles: Problems and Prospects. *Polymers (Basel).* **2021**, *13*, 1–11, doi:10.3390/polym13213759.
73. De Silva, D.A.; Poole-Warren, L.A.; Martens, P.J.; In Het Panhuis, M. Mechanical Characteristics of Swollen Gellan Gum Hydrogels. *J. Appl. Polym. Sci.* **2013**, *130*, 3374–3383, doi:10.1002/app.39583.
74. Far, J.; Abdel-Haq, M.; Gruber, M.; Abu Ammar, A. Developing Biodegradable Nanoparticles Loaded with Mometasone Furoate for Potential Nasal Drug Delivery. *ACS Omega* **2020**, *5*, 7432–7439, doi:10.1021/acsomega.0c00111.
75. Yeh, Y.C.; Huang, T.H.; Yang, S.C.; Chen, C.C.; Fang, J.Y. Nano-Based Drug Delivery or Targeting to Eradicate Bacteria for Infection Mitigation: A Review of Recent Advances. *Front. Chem.* **2020**, *8*, 1–22, doi:10.3389/fchem.2020.00286.
76. Zhang, L.; Jiang, Y.; Ding, Y.; Povey, M.; York, D. Investigation into the Antibacterial Behaviour of Suspensions of ZnO Nanoparticles (ZnO Nanofluids). *J. Nanoparticle Res.* **2007**, *9*, 479–489, doi:10.1007/s11051-006-9150-1.
77. Aruguete, D.M.; Hochella, M.F. Bacteria-Nanoparticle Interactions and Their Environmental Implications. *Environ. Chem.* **2010**, *7*, 3–9, doi:10.1071/EN09115.
78. Yokel, R.A. Direct Nose to the Brain Nanomedicine Delivery Presents a Formidable Challenge. *Wiley Interdiscip. Rev. Nanomedicine Nanobiotechnology* **2022**, *14*, 1–40, doi:10.1002/wnan.1767.
79. Protopapa, C.; Siamidi, A.; Pavlou, P.; Vlachou, M. Excipients Used for Modified Nasal Drug Delivery: A Mini-Review of the Recent Advances. *Materials (Basel).* **2022**, *15*, doi:10.3390/ma15196547.
80. Bastier, P.L.; Lechot, A.; Bordenave, L.; Durand, M.; De Gabory, L. Nasal Irrigation: From Empiricism to Evidence-Based Medicine. A Review. *Eur. Ann. Otorhinolaryngol. Head Neck Dis.* **2015**, *132*, 281–285, doi:10.1016/j.anorl.2015.08.001.
81. England, R.J.A.; Homer, J.J.; Knight, L.C.; Ell, S.R. Nasal PH Measurement: A Reliable and Repeatable Parameter. *Clin. Otolaryngol. Allied Sci.* **1999**, *24*, 67–68, doi:10.1046/j.1365-2273.1999.00223.x.
82. Beule, A.G. Physiology and Pathophysiology of Respiratory Mucosa of the Nose and the Paranasal Sinuses. *GMS Curr. Top. Otorhinolaryngol. - Head Neck Surg.* **2010**, *9*, 1–24, doi:10.1055/s-0029-1246124.
83. Washington, N.; Steele, R.J.C.; Jackson, S.J.; Bush, D.; Mason, J.; Gill, D.A.; Pitt, K.; Rawlins, D.A. Determination of Baseline Human Nasal PH and the Effect of Intranasally Administered Buffers. *Int. J. Pharm.* **2000**, *198*, 139–146, doi:10.1016/S0378-5173(99)00442-1.
84. Kim, B.G.; Kim, J.H.; Kim, S.W.; Kim, S.W.; Jin, K.S.; Cho, J.H.; Kang, J.M.; Park, S.Y. Nasal PH in Patients with Chronic Rhinosinusitis before and after Endoscopic Sinus Surgery.

Am. J. Otolaryngol. - Head Neck Med. Surg. **2013**, *34*, 505–507, doi:10.1016/j.amjoto.2013.04.015.
85. Kumar, R.A.; Viswanatha, B.; Krishnamurthy, N.; Jayanna, N.; Shetty, D.R. Efficacy of Hypertonic Saline and Normal Saline in the Treatment of Chronic Sinusitis. *Int. J. Otolaryngol. Head & Neck Surg.* **2013**, *02*, 90–96, doi:10.4236/ijohns.2013.23022.
86. Liu, L.; Pan, M.; Li, Y.; Tan, G.; Yang, Y. Efficacy of Nasal Irrigation with Hypertonic Saline on Chronic Rhinosinusitis: Systematic Review and Meta-Analysis. *Braz. J. Otorhinolaryngol.* **2020**, *86*, 639–646, doi:10.1016/j.bjorl.2020.03.008.
87. Casale, M.; Moffa, A.; Cassano, M.; Carinci, F.; Lopez, M.A.; Trecca, E.M.C.; Torretta, S.; Rinaldi, V.; Pignataro, L. Saline Nasal Irrigations for Chronic Rhinosinusitis: From Everyday Practice to Evidence-Based Medicine. An Update. *Int. J. Immunopathol. Pharmacol.* **2018**, *32*, 1–6, doi:10.1177/2058738418802676.
88. Culig, J.; Leppée, M.; Vceva, A.; Djanic, D. Efficiency of Hypertonic and Isotonic Seawater Solutions in Chronic Rhinosinusitis. *Med. Glas. (Zenica).* **2010**, *7*, 116–123.
89. Friedman, M.; Vidyasagar, R.; Joseph, N. A Randomized, Prospective, Double-Blind Study on the Efficacy of Dead Sea Salt Nasal Irrigation. *Laryngoscope* **2006**, *116*, 878–882, doi:10.1097/01.mlg.0000216798.10007.76.
90. Kanjanawasee, D.; Seresirikachorn, K.; Chitsuthipakorn, W.; Snidvongs, K. Hypertonic Saline Versus Isotonic Saline Nasal Irrigation: Systematic Review and Meta-Analysis. *Am. J. Rhinol. Allergy* **2018**, *32*, 269–279, doi:10.1177/1945892418773566.
91. Shah, V.; Sharma, M.; Pandya, R.; Parikh, R.K.; Bharatiya, B.; Shukla, A.; Tsai, H.C. Quality by Design Approach for an in Situ Gelling Microemulsion of Lorazepam via Intranasal Route. *Mater. Sci. Eng. C* **2017**, *75*, 1231–1241, doi:10.1016/j.msec.2017.03.002.
92. Kaur, P.; Garg, T.; Rath, G.; Goyal, A.K. In Situ Nasal Gel Drug Delivery: A Novel Approach for Brain Targeting through the Mucosal Membrane. *Artif. Cells, Nanomedicine Biotechnol.* **2016**, *44*, 1167–1176, doi:10.3109/21691401.2015.1012260.
93. Wang, Y.; Jiang, S.; Wang, H.; Bie, H. A Mucoadhesive, Thermoreversible in Situ Nasal Gel of Geniposide for Neurodegenerative Diseases. *PLoS One* **2017**, *12*, 1–17, doi:10.1371/journal.pone.0189478.
94. Verekar, R.R.; Gurav, S.S.; Bolmal, U. Thermosensitive Mucoadhesive in Situ Gel for Intranasal Delivery of Almotriptan Malate: Formulation, Characterization, and Evaluation. *J. Drug Deliv. Sci. Technol.* **2020**, *58*, 101778, doi:10.1016/j.jddst.2020.101778.
95. Kiss, T.; Ambrus, R.; Abdelghafour, M.M.; Zeiringer, S.; Selmani, A.; Roblegg, E.; Budai-Szűcs, M.; Janovák, L.; Lőrinczi, B.; Deák, Á.; et al. Preparation and Detailed Characterization of the Thiomer Chitosan–Cysteine as a Suitable Mucoadhesive Excipient for Nasal Powders. *Int. J. Pharm.* **2022**, *626*, doi:10.1016/j.ijpharm.2022.122188.
96. Yang, J.; Bai, Y.; Sun, J.; Lv, K.; Han, J.; Dai, L. Experimental Study on Physicochemical Properties of a Shear Thixotropic Polymer Gel for Lost Circulation Control. *Gels* **2022**, *8*, 1–23, doi:10.3390/gels8040229.
97. Bonacucina, G.; Cespi, M.; Misici-Falzi, M.; Palmieri, G.F. Rheological, Adhesive and Release Characterisation of Semisolid Carbopol/Tetraglycol Systems. *Int. J. Pharm.* **2006**, *307*, 129–140, doi:10.1016/j.ijpharm.2005.09.034.
98. Abouhussein, D.M.N.; Khattab, A.; Bayoumi, N.A.; Mahmoud, A.F.; Sakr, T.M. Brain Targeted Rivastigmine Mucoadhesive Thermosensitive In Situ Gel: Optimization, in Vitro Evaluation, Radiolabeling, in Vivo Pharmacokinetics and Biodistribution. *J. Drug Deliv. Sci. Technol.* **2018**, *43*, 129–140, doi:10.1016/j.jddst.2017.09.021.
99. Yong, C.S.; Choi, J.S.; Quan, Q.Z.; Rhee, J.D.; Kim, C.K.; Lim, S.J.; Kim, K.M.; Oh, P.S.; Choi, H.G. Effect of Sodium Chloride on the Gelation Temperature, Gel Strength and Bioadhesive Force of Poloxamer Gels Containing Diclofenac Sodium. *Int. J. Pharm.* **2001**, *226*, 195–205, doi:10.1016/S0378-5173(01)00809-2.
100. Qian, S.; Wong, Y.C.; Zuo, Z. Development, Characterization and Application of in Situ Gel

Systems for Intranasal Delivery of Tacrine. *Int. J. Pharm.* **2014**, *468*, 272–282, doi:10.1016/j.ijpharm.2014.04.015.
101. Kolawole, O.M.; Cook, M.T. In Situ Gelling Drug Delivery Systems for Topical Drug Delivery. *Eur. J. Pharm. Biopharm.* **2023**, *184*, 36–49, doi:10.1016/j.ejpb.2023.01.007.
102. Kakati, N.; Parashar, C.K.; Thakur, S.; Deshmukh, O.S.; Bandyopadhyay, D. Microrheology of Mucin-Albumin Assembly Using Diffusing Wave Spectroscopy. *ACS Appl. Bio Mater.* **2022**, *5*, doi:10.1021/acsabm.2c00098.
103. del Castillo-Santaella, T.; Aguilera-Garrido, A.; Galisteo-González, F.; Gálvez-Ruiz, M.J.; Molina-Bolívar, J.A.; Maldonado-Valderrama, J. Hyaluronic Acid and Human/Bovine Serum Albumin Shelled Nanocapsules: Interaction with Mucins and in Vitro Digestibility of Interfacial Films. *Food Chem.* **2022**, *383*, doi:10.1016/j.foodchem.2022.132330.
104. Mardikasari, S.A.; Katona, G.; Sipos, B.; Ambrus, R.; Csóka, I. Preparation and Optimization of Bovine Serum Albumin Nanoparticles as a Promising Gelling System for Enhanced Nasal Drug Administration. *Gels* **2023**, *9*, doi:10.3390/gels9110896.
105. European Medicines Agency (EMA) *ICH Guidelines Q2(R2) on Validation of Analytical Procedures*; 2022; Vol. 2;.
106. Matricardi, P.; Cencetti, C.; Ria, R.; Alhaique, F.; Coviello, T. Preparation and Characterization of Novel Gellan Gum Hydrogels Suitable for Modified Drug Release. *Molecules* **2009**, *14*, 3376–3391, doi:10.3390/molecules14093376.
107. Shelke, S.; Shahi, S.; Jalalpure, S.; Dhamecha, D. Poloxamer 407-Based Intranasal Thermoreversible Gel of Zolmitriptan-Loaded Nanoethosomes: Formulation, Optimization, Evaluation and Permeation Studies. *J. Liposome Res.* **2016**, *26*, 313–323.
108. Akkari, A.C.S.; Papini, J.Z.B.; Garcia, G.K.; Franco, M.K.K.D.; Cavalcanti, L.P.; Gasperini, A.; Alkschbirs, M.I.; Yokaichyia, F.; De Paula, E.; Tófoli, G.R.; et al. Poloxamer 407/188 Binary Thermosensitive Hydrogels as Delivery Systems for Infiltrative Local Anesthesia: Physico-Chemical Characterization and Pharmacological Evaluation. *Mater. Sci. Eng. C* **2016**, *68*, 299–307, doi:10.1016/j.msec.2016.05.088.
109. Balouiri, M.; Sadiki, M.; Ibnsouda, S.K. Methods for in Vitro Evaluating Antimicrobial Activity: A Review. *J. Pharm. Anal.* **2016**, *6*, 71–79, doi:10.1016/j.jpha.2015.11.005.
110. Mardikasari, S.A.; Budai-Szűcs, M.; Orosz, L.; Burián, K.; Csóka, I.; Katona, G. Development of Thermoresponsive-Gel-Matrix-Embedded Amoxicillin Trihydrate-Loaded Bovine Serum Albumin Nanoparticles for Local Intranasal Therapy. *Gels* **2022**, *8*, doi:10.3390/gels8110750.
111. Mardikasari, S.A.; Katona, G.; Budai-Szűcs, M.; Sipos, B.; Orosz, L.; Burián, K.; Rovo, L.; Csóka, I. Quality by Design-Based Optimization of In Situ Ionic-Sensitive Gels of Amoxicillin-Loaded Bovine Serum Albumin Nanoparticles for Enhanced Local Nasal Delivery. *Int. J. Pharm.* **2023**, *645*, doi:10.1016/j.ijpharm.2023.123435.
112. Vigani, B.; Rossi, S.; Sandri, G.; Bonferoni, M.C.; Caramella, C.M.; Ferrari, F. Recent Advances in the Development of in Situ Gelling Drug Delivery Systems for Non-Parenteral Administration Routes. *Pharmaceutics* **2020**, *12*, 1–29, doi:10.3390/pharmaceutics12090859.
113. Wang, S.; Gao, Y.; Jin, Q.; Ji, J. Emerging Antibacterial Nanomedicine For Enhanced Antibiotic Therapy. *Biomater. Sci.* **2020**, *8*, 6825–6839, doi:10.1039/d0bm00974a.
114. Mardikasari, S.A.; Katona, G.; Budai-Szűcs, M.; Kiricsi, A.; Rovo, L.; Csóka, I. Mucoadhesive In Situ Nasal Gel of Amoxicillin Trihydrate for Improved Local Delivery: Ex Vivo Mucosal Permeation and Retention Studies. *Eur. J. Pharm. Sci.* **2024**, *202*, 1–11, doi:10.1016/j.ejps.2024.106897.
115. Bartos, C.; Szabó-Révész, P.; Horváth, T.; Varga, P.; Ambrus, R. Comparison of Modern in Vitro Permeability Methods with the Aim of Investigation Nasal Dosage Forms. *Pharmaceutics* **2021**, *13*, doi:10.3390/pharmaceutics13060846.
116. Elzoghby, A.O.; Samy, W.M.; Elgindy, N.A. Albumin-Based Nanoparticles as Potential Controlled Release Drug Delivery Systems. *J. Control. Release* **2012**, *157*, 168–182, doi:10.1016/j.jconrel.2011.07.031.

9. ACKNOWLEDGEMENT

I would like to thank my supervisor, as well as the head of the Institute, Prof. Dr. Ildikó Csóka, for the guidance, support, and encouragement throughout the entire process of this precious journey. Thank you for giving me the opportunity as Ph.D student at the Institute of Pharmaceutical Technology and Regulatory Affairs. All laboratory facilities, essential materials, and advanced instruments have been invaluable to the successful establishment of this research.

I would like to extend my sincere gratitude to my supervisor, Dr. habil. Gábor Katona, for his patience and dedication. His unwavering belief in my abilities has inspired me to push the boundaries of my academic pursuits. Thank you so much for always being available to answer my questions and providing great support for all my ideas.

I would like to thank all members of the Institute of Pharmaceutical Technology and Regulatory Affairs, especially Prof. Dr. Rita Ambrus, Dr. Mária Budai-Szűcs, and Dr. Bence Sipos, their contribution were truly meaningful for the completion of this research work. I am also grateful to Erika Boda, Béniám Balázs, and Kovács Klára, for always helping me with the instruments during my research investigation. I am also thankful to the administration staff of our institute, Weszelovszkyné Dér Evelyn and Ágnes Balázs, for their assistance with the paperwork, which has ensured the smooth progress of my studies.

I would like to thank all collaboration partners from other departments who helped me in the process towards the success of this research work: Prof. Dr. Katalin Burián and Dr. László Orosz from the Department of Medical Microbiology, Albert Szent-Györgyi Health Center, Albert Szent-Györgyi Medical School, University of Szeged; and also Prof. László Rovó and Dr. Ágnes Kiricsi from the Department of Oto-Rhino-Larynology and Head-Neck Surgery, University of Szeged.

I would like to thank my fellow PhD students and colleagues for their friendship, insightful discussions, and motivation, which have made this journey not only productive but also enjoyable. Lastly, I extend my heartfelt thanks to my parents, my husband, my children, and my sisters for their unconditional help, support, and motivation, which have enabled me to complete my studies.

I acknowledge that the current thesis and other non-related projects were supported by Project no. TKP2021-EGA-32 implemented with the support provided by the Ministry of Culture and Innovation of Hungary from the National Research, Development and Innovation Fund, financed under the TKP2021-EGA funding scheme.

ANNEX